Vibrational energy transfer and migration processes in matrix isolated CH3F

V. A. Apkarian, Lawrence Wiedeman, Willi Janiesch, and Eric Weitz

Citation: The Journal of Chemical Physics **85**, 5593 (1986); doi: 10.1063/1.451574
View online: http://dx.doi.org/10.1063/1.451574
View Table of Contents: http://scitation.aip.org/content/aip/journal/jcp/85/10?ver=pdfcov
Published by the AIP Publishing

Vibrational energy transfer and migration processes in matrix isolated CH_3F

V. A. Apkarian and Lawrence Wiedeman
Department of Chemistry, University of California, Irvine, California 92717

Willi Janiesch and Eric Weitz
Department of Chemistry, Northwestern University, Evanston, Illinois 60201

(Received 7 April 1986; accepted 18 July 1986)

Following excitation of the ν_3 mode in matrix isolated CH_3F, population of $2\nu_3$ is observed. Population of $2\nu_3$ occurs via intermolecular vibration–vibration (V–V) energy transfer driven by the exothermicity of the anharmonic V–V step equilibrating these states. In the equilibration process, both resonant and nonresonant intermolecular energy transfer processes have been identified. The probabilities of each of these processes have been determined. The phonon assisted nonresonant V–V process has a probability of 3.8×10^{-35} and 6.7×10^{-35} $cm^6\ s^{-1}$ in Xe at 10 and 20 K, respectively. These probabilities were obtained from fluence dependent studies of the rise rate of $2\nu_3$ in concentrated matrices. V–V transfer has also been studied in dilute matrices and matrices of intermediate dilution. Signals obtained in these concentration regimes are not exponential but can be reproduced by a Monte Carlo model of V–V transfer. In these matrices there is no longer rapid vibrational energy migration on the time scale of vibrational deactivation. The consequences of the lack of rapid V–V transfer on this time scale are discussed. The difference in energy transfer behavior of CH_3F when excited via ν_3 vs excitation at 3000 cm^{-1} is also rationalized. The temperature dependence and fluence dependence of deactivation rates of ν_3 excited CH_3F are also reported in Ar, Kr, and Xe matrices. By overcoating Ar and Kr matrices with Xe, the temperature range of these measurements has been extended beyond that previously reported.

I. INTRODUCTION

Cryogenic rare gas matrices have already proven to be fruitful media for the study of molecular dynamics.[1] In addition to being an obvious tool for understanding physics and chemistry peculiar to the solid state, intramolecular dynamics common to all states of matter can be probed: light mediated chemistry[2] and mode specific isomerization[3,4] are two notable examples. A common theme that has emerged from studies of chemical dynamics is the need for a more thorough understanding of the disposition of vibrational energy by trapped molecules: intramolecular energy transfer, long-range intermolecular energy transfer, and finally deactivation processes. The significant theoretical and experimental progress made in recent years toward an understanding of deactivation processes in these solids has been summarized in a number of review articles.[5–8] Experimental data is scarcer with respect to intermolecular energy transfer in the ground electronic states of molecules. Systems that have been the subject of detailed experiments include, CO,[5] HCl,[9] HCN,[10] and CH_3F[11–13] trapped in cyrogenic matrices. A fundamental counterpart of these studies, energy migration, remains chiefly in the realm of theoretical studies. The general problems of excitonic transport in solids is a field of very lively theoretical activity with few direct experimental probes. The experimental studies are mainly limited to electronic excitation, where it is normally necessary to resort to picosecond techniques.[14] The experiments to be presented in this paper provide direct information about all aspects of vibrational energy transfer discussed above and in particular provide for direct observation of vibronic migration processes. The vibronic migration process is based on the same principles and formalism that govern excitonic transport in general; however the transfer rates proceed on a much slower time scale than those of electronic excitation and hence provide a substantial experimental simplification.

Energy transfer processes in CH_3F have so far been investigated by three different groups. The earliest report involved double resonance studies in which a pulsed CO_2 laser was used as pump and a cw CO_2 laser was used as a probe.[11] Both lasers were tuned to the ν_3 fundamental transition. The probe laser is then sensitive to the time evolution of population in the molecular ground state. A double exponential growth of absorption in the probe beam was observed. The two exponentials coalesced above 30 K. The slow exponential lifetime was interpreted as the intrinsic relaxation rate of ν_3 and reported to be 250, 333, 87, and 17 ms^{-1} in Ne, Ar, Kr, and Xe. A mild temperature dependence, characteristic of single phonon assistance, was also observed; however it should be noted that the reported values are for 30 K at least in Kr and Xe.[11]

We have previously reported on our laser-induced fluorescence studies of CH_3F and succinctly described the efficient intermolecular *V–V* transfer processes observed in matrix isolated CH_3F.[12] The present paper is an extension of that report. In our laser induced fluorescence studies, ν_3 of CH_3F is excited by a CO_2 laser and fluorescence is observed from the ν_3 overtone, $2\nu_3$. At 10 K the overtone relaxes at 750 ± 70, 160 ± 15, and 20 ± 3 ms^{-1} in Ar, Kr, and Xe, respectively. At 30 K in Kr and Xe the relaxation rates are 190 and 32 ms^{-1}. These rates can be compared to the relaxation rates at 30 K from Ref. 11, that are cited above. When this is done, it is apparent that the relaxation of $2\nu_3$ is, within experimental error, twice the relaxation rate of ν_3, More-

over, the $2\nu_3$ relaxation was observed to follow the same concentration, temperature, and host dependencies as ν_3, indicating efficient V–V exchange processes equilibrating these two states through the energy pooling mechanism:

$$CH_3F(\nu_3) + CH_3F(\nu_3) \underset{k_b}{\overset{k_f}{\rightleftarrows}} CH_3F(2\nu_3) + CH_3F(\text{gnd}) \quad \Delta E = -16\ \text{cm}^{-1}. \tag{1}$$

The doubling of relaxation rates of $2\nu_3$ vs ν_3 can be nicely explained by the above mechanism alone as long as k_f and k_b are larger than the relaxation rate constant of ν_3, k_r. It is worth noting, however, that since k_b describes an endoergic process, it will tend to zero in the limit of 0 K. Thus, at very low temperatures the assumption of fast equilibrium between ν_3 and $2\nu_3$ cannot be maintained by the scheme of Eq. (1) alone.

More recently, laser-induced fluorescence experiments were reported, in which the 3 μm region of the CH_3F vibrational manifold was initially excited and fluorescence could only be observed from $2\nu_3$ and ν_3.[13] The observed rates were explained by a rapid sequential intramolecular relaxation without invoking intermolecular transfer:

$$CH_3F(3\,\mu) \rightarrow CH_3F(2\nu_3), \tag{2a}$$

$$CH_3F(2\nu_3) \overset{k_{21}}{\rightarrow} CH_3F(\nu_3), \tag{2b}$$

$$CH_3F(\nu_3) \overset{k_r}{\rightarrow} CH_3F(\text{ground}). \tag{2c}$$

In these experiments, the time evolution of populations of $2\nu_3$ was directly monitored by detecting fluorescence from $2\nu_3 \rightarrow$ gnd. The population in $2\nu_3$ rises within the laser pulse and falls at 320 ± 40, 88 ± 10, and 13 ± 2 ms^{-1} in Ar, Kr, and Xe, respectively, at 10 K. The $\nu_3 \rightarrow$ gnd fluorescence could not be separated from the $2\nu_3 \rightarrow \nu_3$ emission. Thus the observed 10μ emission was carefully analyzed as a sum of an exponential fall and exponential rise–fall weighted by the Einstein coefficients of the two transitions. The argument for the absence of any intermolecular energy transfer by the mechanism of Eq. (1) was based on a comparison of amplitudes of $2\nu_3$ and ν_3 emissions in the sum signal. Thus it was concluded that the direct relaxation of $2\nu_3$, as in Eq. (2b), was more efficient than the relaxation of ν_3 ($k_{21} \sim 4k_r$ in Ar and Kr).

In the present paper we report in detail our experimental findings and reconcile the seemingly different conclusions derived in the previous reports. A kinetic analysis will be employed to describe the time dependence of the state populations via different methods of preparation and probing employed by the different studies. However, the standard formulations of rate equations employed in chemical kinetics is in general, inappropriate for treatments of energy transfer in solids since in general, it may not be possible to define rate constants. Rate constants are defined as

$$k = \frac{\langle P \rangle}{C^n},$$

in which $\langle P \rangle$ is the ensemble average of the microscopic probability of a given process, C is a concentration, and n is the molecularity of the process. Such a constant can only be obtained if $\langle P \rangle$ is time independent and has exactly a C^n dependence. However, approximate rate constants can be defined under specific conditions. In the first part of the discussion the relationship between macroscopic rates and microscopic probabilities are considered. The kinetic treatment is then presented in the appropriate regime. A probabilistic approach is taken for the interpretation of observations in dilute matrices in which the kinetic treatment is unacceptable.

II. EXPERIMENTAL

The details of the experimental setup have been previously reported.[12] Briefly, a commercial, closed-cycle cryostat (Air Product Displex 202) is used for the preparation of matrices. The system is maintained under high vacuum, 10^{-7} Torr, throughout the experiments. However, small bursts of pressure are observed during deposition as a consequence of the pulsed deposition technique used in the preparation of the matrix. The matrix is irradiated by a Q-switched CO_2 laser whose operating parameters have been previously described.[12] However, an important point is that its pulse width was between 0.5–1 μs. Fluorescence is collected through an appropriate interference filter by an In:Sb detector. The signals are averaged and sent to a computer for analysis and storage. The cryostat and vacuum manifold were mounted on a cart and could be made to access an FTIR spectrometer. High resolution spectra obtained by this system have already been reported.[15]

Laser-induced fluorescence data were typically studied as a function of concentration, temperature, and laser fluence. Gas mixtures were prepared in an all metal manifold and pressures were measured by a capacitance manometer. The rare gases used were of research grade purity, 99.9999% as specified by the manufacturer, and were used without further purification. CH_3F was obtained at 99.0% purity and further purified by multiple freeze–pump–thaw cycles prior to use. No evidence of contamination was discerned in the spectroscopic studies which spanned a wide range of concentrations: $M/R = 500{:}1$ to $M/R = 100\,000{:}1$. The range of temperatures studied in this experiment was 9 K at the lower limit, determined by the cooling capacity of the cryostat, and at the upper limit it was determined by the melting point of the matrix. In the case of Ar and Kr matrices an overcoat of pure Xe increased the upper temperature limit. Thus in the case of Xe overcoated Kr matrices it was possible to make measurements at temperatures as high as 72 K without substantial loss of matrix material and with subsequent measurements at lower temperatures unaffected by this temperature cycle. Fluence dependent studies were performed by inserting polyethylene films in the laser beam. The method yielded a limited range of fluences, ~ 0.3–2 mJ/cm^2, however it guaranteed spatial and temporal uniformity. Fluorescence signals were analyzed by an iterative Guggenheim algorithm which has been previously discussed.[16]

III. RESULTS

Upon excitation of the ν_3 mode of CH_3F with a CO_2 laser, 5 μm fluorescence was detected with a large element,

~ 1.5 cm diameter, In:Sb detector (long wavelength cutoff at 6 μm). The time evolution of the fluorescence collected through a 4.8 μ long-pass filter [with this filter the effective bandpass of the detector becomes 4.83–5.67 μm (5% pts)] was essentially identical to that for unfiltered detection and degradation of signal intensity through the filter could be accounted for by transmission losses of the filter. A 4.7 μ bandpass filter (producing an effective bandpass of 4.69–4.89 μ) reduced the signal by a factor of 250 while a 3–4 μ bandpass filter (with an effective bandpass of 3.01–4.00 μ) essentially eliminated the fluorescence. Thus no direct emission could be observed from ν_1 and ν_4 in the 3000 cm^{-1} region. A Au:Ge detector was used to search for emission from ν_2 and ν_5 states in the 1500 cm^{-1} region, however no emission for these states could be detected. Thus no emission could be detected from many of the states that are prominent in gas phase LIF studies.[17] The only observed emission could be attributed to overtone emission from the ν_3 manifold. The spectral composition of the 5 μ emission was further scrutinized by detection of fluorescence through a circularly variable interference filter (CVF). A resolution of 30 cm^{-1} was attained by the system using 1° slits. This was verified by IR spectra of the filter–slit combination. However, due to mismatch of slit size to detector element size, and in the absence of corrective optics, the detection sensitivity of the arrangement was reduced by 50-fold relative to the unfiltered detection. At this reduced sensitivity, $> 10^6$ averages were necessary to obtain a signal-to-noise (S/N) ratio of ~ 5. Yet it was possible to establish that in Xe matrices, where the $2\nu_3$ absorption had been directly observed in IR spectra at 2044 cm^{-1}, the fluorescence rise rates and intensities were the same with the CVF centered at 2044 and 2025 cm^{-1}. Signals were approximately half as intense at 2025 cm^{-1} which produced signals that had sufficiently low S/N ratios that they were difficult to analyze. However, signals appeared slower when the CVF was set at 2065 or 1810 cm^{-1} than when the CVF was centered at 2044 or 2025 cm^{-1}. The excellent match of the peak emission with the $2\nu_3$ absorption frequency and the excellent agreement of the time dependence of unfiltered emission with $2\nu_3$ emission allows us to conclude that $2\nu_3$ fluorescence dominates the emission spectrum. Thus in the majority of experiments fluorescence was detected using an unfiltered InSb detector.

It appears unlikely that the emission observed at frequencies other than where $2\nu_3$ emission is expected is due to $3\nu_3$ or higher overtones in the ν_3 manifold. As will be discussed later, kinetic considerations would argue that even if $3\nu_3$ was populated in these experiments, energy transfer to the nearby 3 μ states would preclude the attainment of any significant steady state population and hence preclude its observation through direction emission. Emission from phonon sidebands is possible and though the conclusion is speculative we are forced to conclude that this is the major source of emission at frequencies other than where $2\nu_3$ absorbs.

The observed rise of fluorescence intensity is delayed relative to the excitation pulse width, especially in Xe matrices. Thus direct two-photon excitation of the overtone state is eliminated as a possibility. This is further verified by power dependent studies to be described below. Moreover, as will be elaborated on in the Discussion section, since the overtone relaxation rate is always twice the relaxation rate of the fundamental state, the mechanism of overtone excitation can confidently be attributed to the energy pooling process of Eq. (1). It is important to note that this process involves simultaneous intramolecular and intermolecular vibrational energy transfer steps. In order to determine the details of this V–V process, the rise rate of fluorescence was studied in different matrices and as a function of temperature, concentration, and laser fluence. Xe matrices were investigated most extensively for this purpose since the rise rates were slowest in these systems and were unaffected by the electronic response time of the detection system. Very few experiments were performed in Ar matrices because of the fast rates of rise and limited temperature range available. In what follows, the experimental results are summarized separately for each matrix material.

A. Xenon

As shown in Fig. 1, the ν_3 absorption of CH_3F in Xe matrices is bracketed by the $P(36)$ and $P(38)$ transitions of the CO_2 laser. Thus ν_3 could be efficiently excited by either line. A typical fluorescence signal obtained from an $M/R = 2500$ sample is shown in Fig. 2. The rise and decay of fluorescence in this sample can be fit satisfactorily by single exponentials and both rates are slow in comparison to the 0.5–1 μs FWHM excitation pulse. Due to the slower rates of rise and fall in Xe as compared to Ar and Kr matrices, more detailed observations and more accurate measurements could be made for this system. Samples of $M/R = 1000$ to $M/R = 100\,000$ were studied and the effects of temperature, laser fluence, and annealing were observed. Concentration and temperature dependence of relaxation rates in these ma-

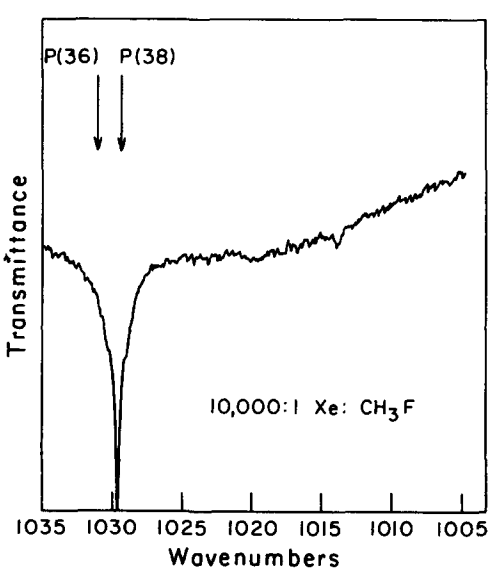

FIG. 1. IR absorption spectrum of CH_3F isolated in a Xe matrix ($M/R = 10\,000$), deposited at 32 K and recorded at 9 K without annealing. The frequencies of the CO_2 laser transitions, $P(36)$ and $P(38)$ of 9.6 μ band used in the LIF studies are indicated by arrows.

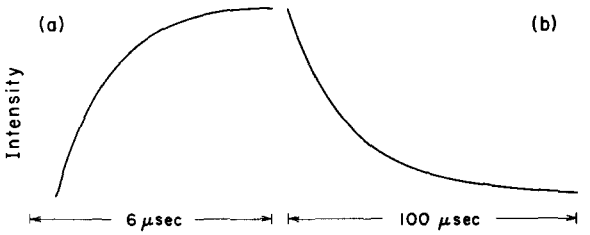

FIG. 2. The smoothed trace of the experimental rise (a) and fall (b) of fluorescence obtained from $2\nu_3$ of CH_3F isolated in Xe ($M/R = 2500$), $T = 9$ K, excitation energy = 1 mJ at $P(36)$. Note the split time scale.

trices have previously been reported. We note here that even in matrices of the highest dilution, $M/R = 100\,000$, vibrational relaxation remains a single exponential for the most part and only in the most concentrated matrices, where extensive aggregation is spectroscopically observed such as in $M/R = 1000$, does vibrational relaxation become biexponential due, as will be discussed, to transfer to dimers and multimers.

In concentrated matrices, $M/R < 7000$, the rise of fluorescence is single exponential and its rate has a linear temperature and fluence dependence (see Figs. 3 and 4). As illustrated in Fig. 5, at intermediate dilutions, $M/R = 10\,000$, the rise contains two components. The first part of this signal is too fast for accurate measurements. However, the slow portion is exponential, maintains a linear temperature and fluence dependence with slopes similar to the single exponential rise rates in concentrated matrices (see Figs. 2 and 3). In dilute matrices, $M/R > 30\,000$, the rise clearly splits into two parts. While the slow part can still be treated as an exponential, it is clear that the fast part cannot be. In Fig. 6 the time evolution of fluorescence observed at different dilutions is shown. In dilute matrices, where the rise is dominated by the fast component, it is difficult to obtain a rate for this rise since it is not exponential. However,

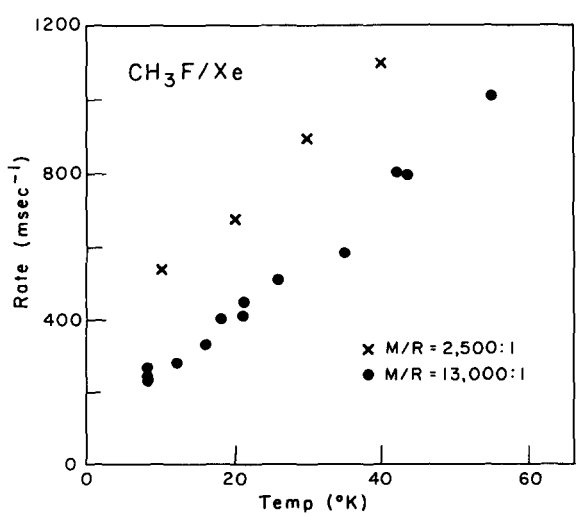

FIG. 3. Temperature dependence of $2\nu_3$ fluorescence rise rates in xenon matrices. Excitation energy, 1 mJ per pulse.

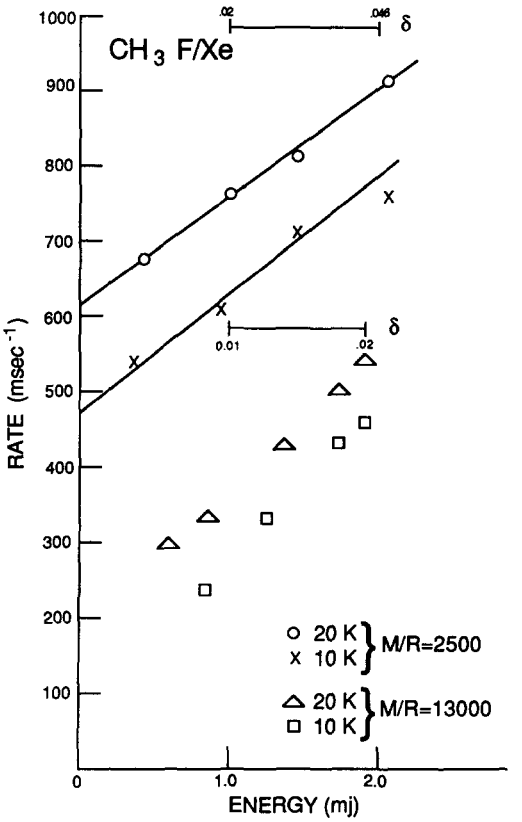

FIG. 4. Fluence dependence of $2\nu_3$ fluorescence rise rates in xenon matrices. The meaning of δ is explained in the text. The top set of numbers for $\delta(0.02 \rightarrow 0.046)$ refer to the 2500:1 matrix while the bottom set $(0.01 \rightarrow 0.02)$ refers to the 13 000:1 matrix.

it is possible to measure the relative amplitude of the fast and slow components as a function of annealing and fluence as illustrated in Fig. 7. It is possible to deduce from Fig. 7 that the fast component is second order in laser fluence while the slow component is linear. In addition, the relative contributions of the fast and slow components are a function of dilution: the larger the dilution, the larger the contribution of the fast component. Thus at dilutions of $\geqslant 1{:}60\,000$ (see Fig. 6), the fluorescence essentially rises with the fast component, and remains flat until the onset of the exponential decay. The overall signal can then be described as having a "flat top."

B. Krypton

In Kr matrices, ν_3 of CH_3F could be excited by numerous CO_2 laser lines. The spectroscopic details have previously been published.[15] The strongest signals were obtained with the $P(32)$ line of the 9.6 μm branch, at 1035.52 cm^{-1}. Weaker fluorescence obtained by excitation with the $P(28)$, $P(30)$, and $P(34)$ lines showed a similar temporal evolution. The fluence dependence of the rise rates were weak while the fall rates were independent of fluence over the M/R range studied. Experiments were performed on samples of different concentrations ranging from $M/R = 1000$ to $M/R = 50\,000$. The deactivation rates at dilutions above 1:7000 were independent of concentration and their temperature dependence were in excellent agreement. The temperature dependence of these rates has previously been reported,

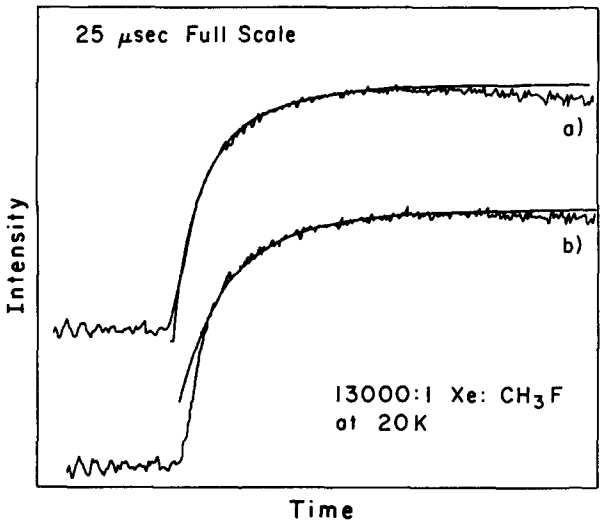

FIG. 5. (a) Double exponential fit, (b) single exponential fit, to the fluorescence rise rate observed in matrices of intermediate dilution ($M/R = 13\,000$).

however the temperature range has now been extended to 72 K by use of a Xe overcoat. In Fig. 8, the deactivation rates obtained from different M/R matrices with $M/R > 7000$ is plotted as a function of temperature. These rates are independent of laser fluence. In more concentrated matrices, the fall rates are faster and show a mild fluence dependence. In Fig. 9 the temperature and fluence dependence of the fall rate from a sample of $M/R = 1250$ is shown. The fluence dependence is nearly linear at 30 $ms^{-1}\,mJ^{-1}\,cm^{-2}$. The rates measured by excitation with $P(28)$, $P(30)$, $P(32)$, and $P(34)$ were in good agreement. When irradiated with $P(38)$ and $P(40)$, which overlap the dimer absorptions, a very weak signal was observed with an instantaneous rise and near response time limited fall.

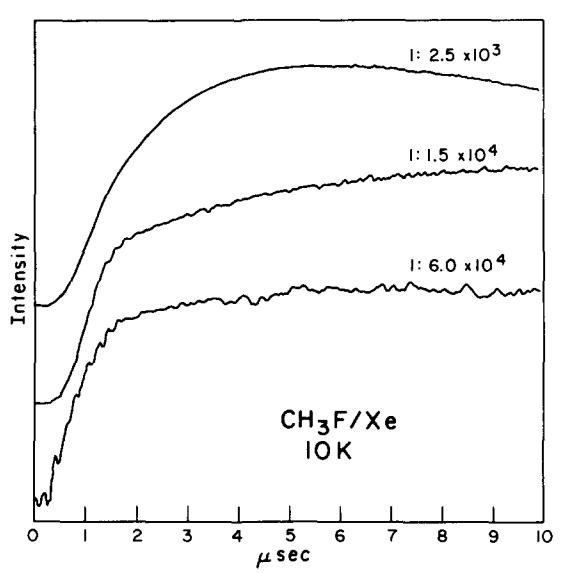

FIG. 6. Experimental traces of the fluorescence rise in xenon matrices of different dilutions, $M/R = 2500$, 15 000, and 60 000 in descending order.

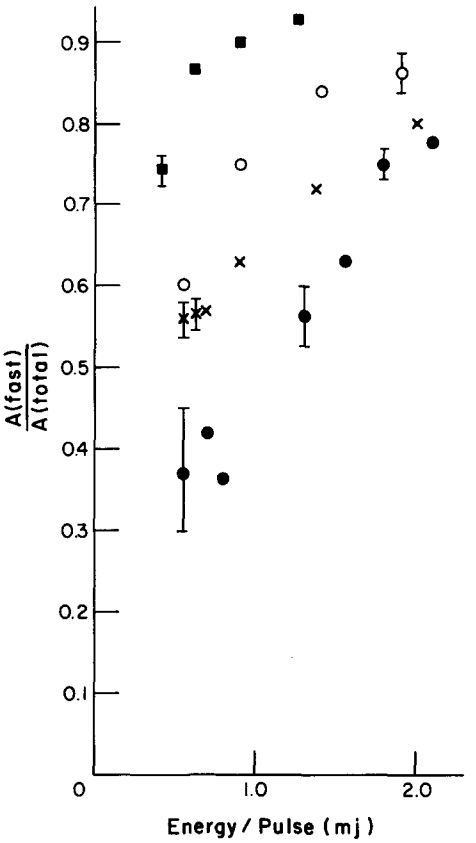

FIG. 7. The ratios of the amplitudes of the fast rise to the slow rise of fluorescence plotted vs the excitation energy. Data taken from a 14 000:1, Xe:CH_3F matrix. (●) at 10 K prior to annealing excited by $P(36)$ of 9:6 μ CO_2 laser line, (X) at 10 K after annealing the sample of 45 K (○) same but at 28 K, (□) same as (X) however excited with $P(38)$.

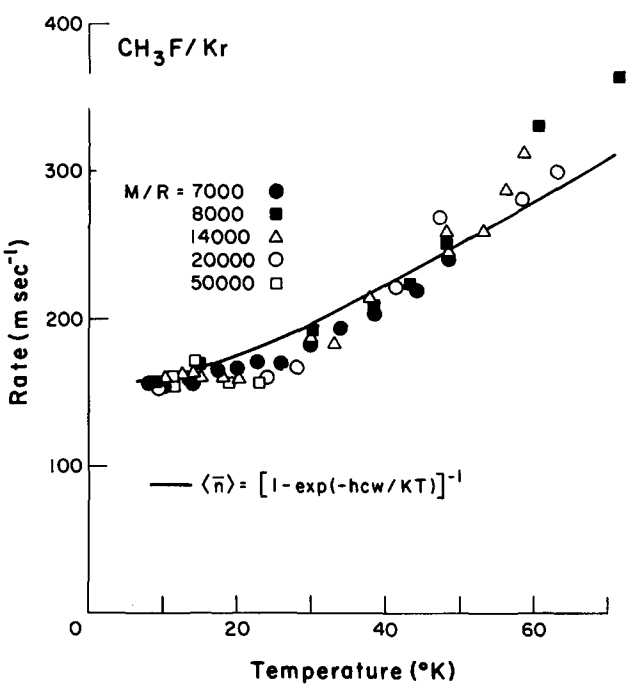

FIG. 8. A compilation of $2\nu_3$ relaxation rates as a function of temperature obtained from Kr matrices of dilutions ranging from $M/R = 7000$ to $M/R = 50\,000$. In matrices of concentration larger than 7000:1 the fall rates become faster due to transfer to dimers. The filled squares were obtained from Kr matrix overcoated with Xe which enabled measurement to be made at temperatures as high as 74 K. The curve that is drawn in has the functional form $[1 - \exp(-hc\omega/kT)]^{-1}$.

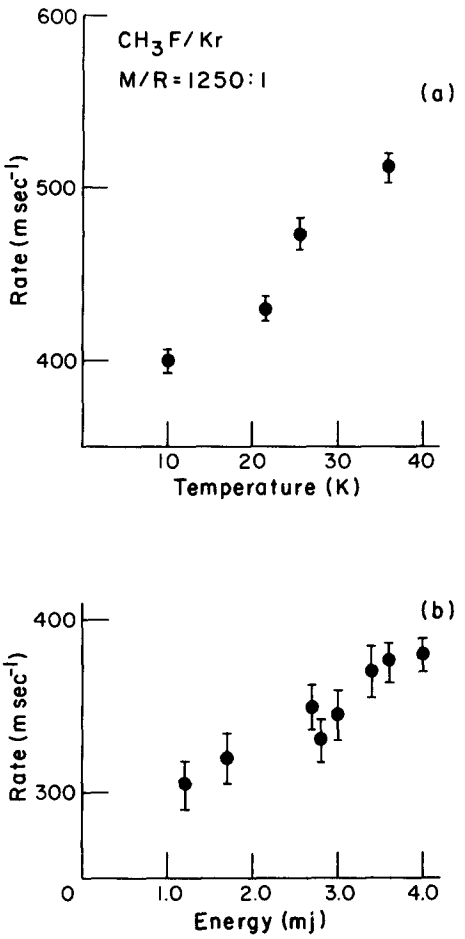

FIG. 9. (a) Temperature dependence of the $2\nu_3$ relaxation rate in a concentrated krypton matrix, $M/R = 1250$. Note the much faster rates in this case relative to those in Fig. 8. (b). The relaxation rate in concentrated matrices ($M/R = 1250$ in Kr) also shows a finite fluence dependence.

In Fig. 10 the fluorescence signal obtained from a sample of $M/R = 7000$ is shown fit to an exponential rise and fall calculated by a nonlinear least-squares routine. The fluorescence rise of $2\nu_3$ in Kr matrices is fast and close to the excitation pulse width of $\leqslant 1\,\mu$s and only a factor of ~ 3 faster than the fall. Thus an initial induction period, due to the finite excitation time, contributes to the rise of the fluorescence.

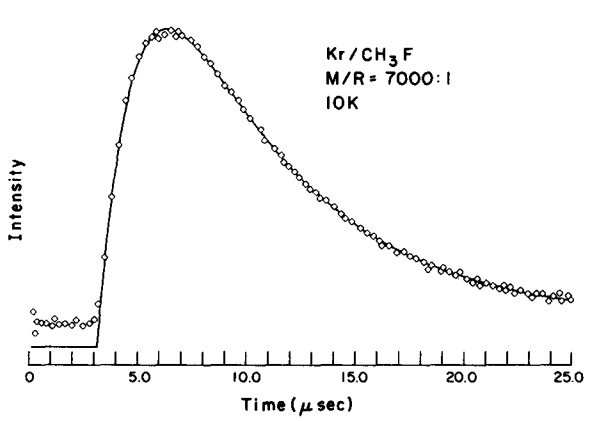

FIG. 10. A trace (□) of the fluorescence observed from $2\nu_3$ in Kr isolated CH_3F, $M/R = 700$, $T = 10$ K. The connecting line is the double exponential fit.

This effect coupled with the convolution of the fall rate with the rise, introduces a large uncertainty to the measured rise rates, ignoring the points belonging to the induction period. The signals were fit to an exponential rise and an exponential fall. The rise rates thus obtained show only a slight increase with temperature and fluence. A rate of 750 ± 50 ms^{-1} is reported as a temperature averaged representative rate of the rise at a fluence of 1.5 mJ/cm^2 for $P(32)$ excitation.

C. Argon

A limited set of experiments were performed in Ar matrices due to the small range of accessible temperatures in our systems and due to the observed near response-time limited rise rates. In Fig. 11 the time evolution of fluorescence from $2\nu_3$ of CH_3F in an Ar matrix is shown. The sample, $M/R = 8500$, was deposited at 9 K and overcoated with a layer of pure Xe. In these experiments, ν_3 was excited by the $P(28)$ line of the CO_2 laser at 1039 cm^{-1}. While the rise rates were near response-time limited, the fall rates could be obtained by fitting the long time decay to a single exponential. At short times—1–3 μs after the fluorescence maximum is attained the decay falls at a slower rate than at longer times. Note the decay cannot be treated as a double exponential fall, since in such a situation the early fall would have to be faster than the later one, nor can the whole time evolution be satisfactorily fit by an exponential rise and an exponential fall. Thus for obvious reasons signals such as those in Fig. 11 are referred to as flat tops. The best exponential fit to the long-time decay is also shown in Fig. 11. The rate obtained is 760 ± 50 ms^{-1} at 20 K. The temperature dependence of the fall rates is shown in the upper panel of Fig. 11.

IV. DISCUSSION

In these experiments, since initially only ν_3 is excited, the observation of any fluorescence in the 2000 cm^{-1} region is contingent upon having an efficient energy transfer mechanism to populate $2\nu_3$. As discussed in Ref. 12 the only effective mechanism that could populate $2\nu_3$ is that of Eq. (1). There remains the possibility that this mechanism is operative only among special reaction centers, such as dimers—which are known to exist in greater than statistical concentrations.[15] This possibility can be disproved by two observations: (a) a very weak transient, with response limited rise and fall, was observed in the 2000 cm^{-1} region when the dimer absorption was directly irradiated in Kr matrices. This is direct evidence to the effect that vibrational relaxation in dimers is more efficient than intermolecular transfer. (b) The relaxation rates of both ν_3 and $2\nu_3$ increase as a function of concentration and in matrices of $M/R < 100$ fluorescence is completely quenched. This is a direct indication to the effect that dimers act as sinks of vibrational excitation. The dependence of rise rates on concentration and laser fluence also agree with this conclusion and will be further discussed. Reaction centers where two molecules are nearer each other than the average statistical intermolecular separation should not be considered special as long as the molecules are spatially isolated. As will be discussed, microscopic probabilities of energy transfer are strongly biased toward

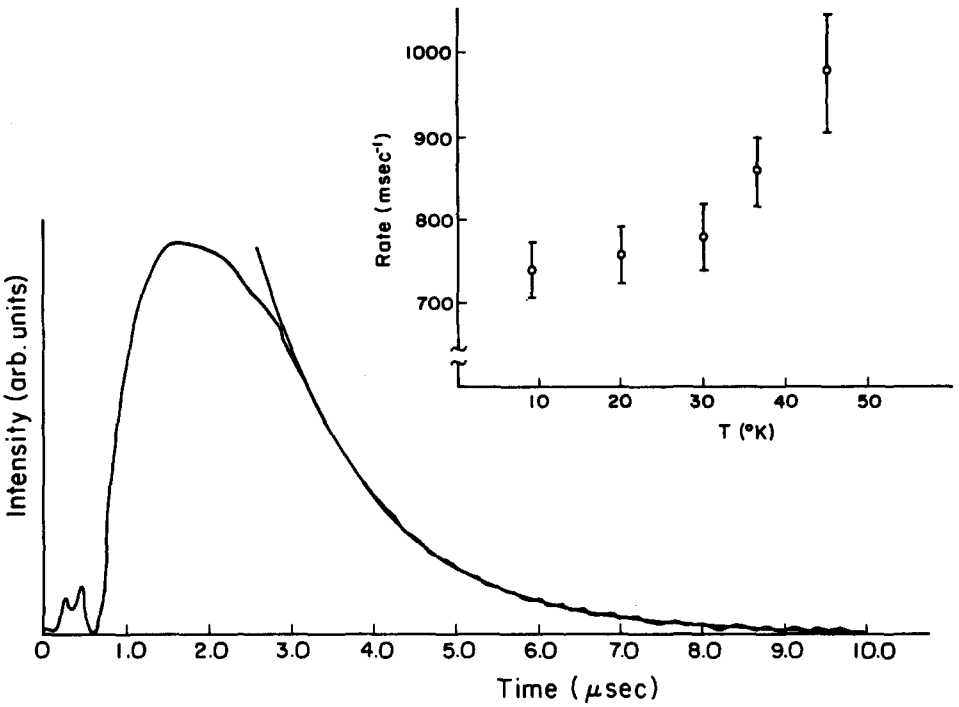

FIG. 11. Fluorescence observed from $2\nu_3$ of CH_3F isolated in an Ar matrix ($M/R = 8500$), showing the "flat top" behavior discussed in the text. In the inset the relaxation rate is plotted as a function of temperature.

such centers through an R^{-6} distance dependence, and the nonresonant V–V transfer of Eq. (1) will be shown to predominantly proceed at such "trap sites," especially in dilute matrices. However, the number of intervening host atoms necessary to consider the molecules to be isolated is not clear. It is known that annealing produces aggregation, and hence it can safely be assumed that in annealed matrices molecules in neighboring cages dimerize and hence are eliminated from the observed ensemble. Explicit effects of annealing on the distribution of guest molecules, and thus on V–V transfer, will be considered in more detail later in this section.

The driving force for the reaction of Eq. (1) is the tendency of molecules to establish a vibrational thermal equilibrium: the "Treanor" effect.[19] It is well known from gas phase experiments that a single vibrational temperature may not be sufficient to describe the populations of different modes (or states) in polyatomic molecules. This effect is expected to be even more pronounced for molecules trapped in low-temperature environments.[20] An added complication is that a single temperature may not even be sufficient for the description of the population in a given mode throughout the matrix. In fact, under conditions of "complete isolation" of molecules, the notion of a vibrational temperature is undefined. Complete isolation in this case is defined as separation of molecules from each other at a large enough distance such that communication between their vibrational states via long-range energy transfer is slower than deactivation.

On a microscopic level, vibrational equilibrium in the systems under study is effected by two major transfer mechanisms, (a) resonant energy transfer, or excitation hopping:

$$CH_3F(\nu_3) + CH_3F(0) \rightleftarrows CH_3F(0) + CH_3F(\nu_3)\,, \quad \Delta E \sim 0\,, \tag{3}$$

where the small deviation from $\Delta E = 0$ is due only to environmental anisotropy and is of the order of the inhomogeneous linewidths in the system (FWHM < 0.1 cm^{-1} in well annealed Kr matrices). (b) The long range energy pooling mechanism of Eq. (1) where both intra- and intermolecular exchange occur simultaneously and the anharmonicity mismatch of ~ 16 cm^{-1} is dissipated by phonons. This process is expected to be less efficient than the resonant hop of Eq. (3) due to the energy gap and the necessity of phonon mediation; thus the processes of Eq. (3) are of longer range (the distance an excitation can travel within its lifetime) than those of Eq. (1).

In a regime where the average separation between two excited molecules is small relative to the range of the nonresonant transfer of Eq. (1), vibrational thermal equilibrium governed by the initial excited state population can be achieved and equilibration processes can, to a very good approximation, be treated by simple equilibrium kinetics, as was done in our previous report.[12] The observed rate of rise in the population of $2\nu_3$ would then directly reflect the microscopic probability of nonresonant energy transfer at an average separation. Thus, this regime will be characterized by exponential evolution of population in the different states. In a regime where the average separation between excited pairs is large relative to the range of the nonresonant process of Eq. (1), overtone population can only be achieved after a pair of excitations meet via the resonant hopping process of Eq. (3) or by being created near each other. In this regime the population evolution of $2\nu_3$ would directly reflect the excitation migration dynamics. As long as the range of resonant energy transfer is larger than the CH_3F intermolecular separations, the excited state population can form a thermodynamic ensemble and achieve a well-defined vibrational temperature.

However, this regime, corresponding to exponential population evolution, occurs under a very limited set of conditions. In general the time evolution will not be described as an exponential and the migration process cannot be described by a simple diffusion model, due to the R^{-6} dependence of the transfer probability. The migration (random walk) of a given excitation will be strongly biased by the initial distribution of the molecules in the lattice and the stepsize will be a strong function of time.[21] Migration in these systems resembles a diffusive process with a strong "memory" and is therefore better described by percolative models.[22] Experimentally, dilute matrices will be characterized by nonexponential evolution of populations. It is important to emphasize that in such a regime a simple equilibrium rate kinetics treatment is not justifiable since equilibrium statistical averages are not applicable. The transition to a regime where vibrational thermal equilibrium can be achieved will depend solely on the relative ranges of the resonant and nonresonant transfer processes of Eqs. (3) and (1). Experimentally, the different regimes can be attained by varying the initial guest/host ratio. We have performed experiments on CH_3F isolated in rare gas matrices over a range of concentrations (1/1000 to 1/100 000) which spans these different regimes. In concentrated systems, simple kinetic models can be applied to obtain microscopic rates of V–V transfer. In more dilute systems, simulations have been performed which confirm our qualitative understanding of the processes that are occurring and which indicate the prospects of using these systems for unraveling the special problems of excitonic migration, and transport phenomena.

A. Microscopic probabilities

The dominant interaction that can induce efficient energy transfer among spatially isolated oscillators is due to dipole–dipole forces. A convenient, however approximate, treatment of this interaction is afforded by the well known Förster–Dexter spectral overlap formalism.[7] This formalism can be derived by assuming that a donor dipole relaxes by emitting a virtual photon which in turn is absorbed by an acceptor dipole located at a distance R_{DA}. The probability for transfer between a donor and an acceptor P_{DA} is given as

$$P_{DA} = C_{DA}/R^{6}_{DA} = \frac{3}{512\pi^6 c n^4 \nu^6 R^{6}_{DA}} \frac{1}{\tau_D} \frac{1}{\tau_A} \int f_D(\nu) f_A(\nu) d\nu , \tag{4}$$

in which c is the speed of light, n the index of refraction of the medium, ν is the transition frequency, R_{DA} is the distance between donor and acceptor, τ_D and τ_A are radiative lifetimes of the donor and acceptor, respectively, $f_D(\nu)$ is the emission line shape of the donor, and $f_A(\nu)$ is the absorption line shape of the acceptor.

In the case of CH_3F molecules excited to ν_3, two types of energy transfer probabilities need be considered: (a) resonant energy transfer between a ν_3 excited molecule, the donor, and a ground state molecule, the acceptor, as in Eq. (3). (b) The energy pooling mechanism in which both donor and acceptor are ν_3 excited molecules as in Eq. (1). The process of Eq. (3) does not produce a change in the vibrational population of the system, it merely serves as a mechanism for the hopping of excitation from one CH_3F occupied site to another. This step is usually referred to as donor–donor (D–D) transfer in the literature, yet it should be noted that the donor and acceptor differ by one being excited and the other not being excited. To avoid confusion we will refer to this step as the "hopping" mechanism. Vibrational populations are changed by the energy pooling mechanism of Eq. (1). This type of energy transfer is referred to as D–A transfer in the literature, yet in this case both donor and acceptor are the same type of species, namely ν_3 excited molecules. The energy mismatch in this case is due to the molecular anharmonicity, $\Delta E = 16\ \mathrm{cm}^{-1}$. Thus this step will be referred to as "nonresonant energy transfer."

Equation (4) is particularly useful for describing energy transfer in systems where emission and absorption line shapes overlap. It is thus adequate for describing the resonant hopping probability. Moreover, this expression can be rigorously evaluated in this case since all the necessary spectroscopic parameters have been determined experimentally. The ν_3 absorption line shape can be approximated as Lorentzian even though it is known to be inhomogeneously broadened at lower temperatures.[15] In the case of exact overlap of two Lorentzians, the integral in Eq. (4) reduces to $(\pi\Delta\nu)^{-1}$. However, the linewidth in matrices is strongly dependent on the method of sample preparation and also strongly temperature dependent. As an example, in a well-annealed Kr matrix, the ν_3 absorption linewidth varies an order of magnitude between 10–40 K.[15] Hence, the Förster probability of resonant energy transfer will vary approximately an order of magnitude over this temperature range. Careful measurement of the integrated absorption coefficient of ν_3 in Kr indicates that within experimental error the radiative lifetime remains the same as the gas phase value.[15] Thus by taking $\tau = 70$ ms, $n = 1.28$, $\nu = 1035\ \mathrm{cm}^{-1}$, $\Delta\nu = 0.1\ \mathrm{cm}^{-1}$ at 10 K, and $1\ \mathrm{cm}^{-1}$ at 40 K, the hopping probability constant can be derived as $C_{hop} = 4\times10^{-32}\ \mathrm{cm}^6\ \mathrm{s}^{-1}$ at 10 K and $4\times10^{-33}\ \mathrm{cm}^6\ \mathrm{s}^{-1}$ at 40 K in Kr matrices. In our Xe matrices, the linewidths were usually determined by inhomogeneous widths of the order of $1\ \mathrm{cm}^{-1}$, throughout the temperature range. This is a reflection of the poorer crystallinity of these matrices as also verified by their highly scattering nature. Thus little temperature variation for the probability of a hop is expected in Xe matrices, and the probability would be expected to be very similar to that for the krypton matrices at 40 K, $4\times10^{-33}\ \mathrm{cm}^6\ \mathrm{s}^{-1}$.

As a first approximation, the nonresonant energy transfer process of Eq. (1), can also be treated by the Förster formalism of Eq. (4). With the assumption of Lorentzian line shapes, the overlap integral can be evaluated as

$$\int f_D(\upsilon) f_A(\upsilon) d\upsilon = \frac{1}{2\pi} \frac{\Delta\nu_D + \Delta\nu_A}{(\nu_D - \nu_A)^2 + (\Delta\nu_D{}^2 + \Delta\nu_A{}^2)/2} = \frac{1}{2\pi} \frac{2\Delta\nu_3}{(\nu_{\nu_3 \to 0} - \nu_{2\nu_3 \to \nu_3})^2} \tag{5}$$

which ranges from 1.2×10^{-4} to 1.2×10^{-3} between 10–40

K in Kr. The latter value can again be assumed as representative of the case in Xe. The Förster probability for the nonresonant transfer of Eq. (1) could then be numerically evaluated in the harmonic approximation, i.e., $\tau_{2\nu_3\to\nu_3} = 2\tau_{\nu_3\to 0}$. However, it is more convenient to consider the ratios of resonant to nonresonant probabilities of transfer, which can be obtained from the appropriate equations as

$$P^{\nu_3\to 0}_{0\to\nu_3}/P^{\nu_3\to 0}_{\nu_3\to 2\nu_3} = 2\frac{(\nu_D-\nu_A)^2}{\Delta\nu^2} = 2\frac{(\nu_{\nu_3\to 0}-\nu_{2\nu_3\to\nu_3})^2}{\Delta\nu^2} \quad (6)$$

which ranges between 5×10^4–5×10^2 for $\Delta\nu = 0.1$ and 1 cm^{-1}, respectively. Not surprisingly, this formulation predicts that the relative efficiencies of the two processes are determined by the spectral overlaps, and hence at low temperatures, where absorption lines are narrowed, the nonresonant process would be expected to have a much lower probability.

However, this model does not include the role of phonons and a more appropriate formulation to treat this process would have to include phonon assisted V–V processes. Therefore the use of the Förster model to evaluate the rates of the nonresonant transfer can be regarded as a lower limit for nonresonant transfer probabilities. A theory has been advanced for the case of phonon assisted V–V transfer in diatomics by Blumen, Lin, and Manz, who demonstrated the Förster expression to be an approximate limit of their more general formulation.[23] According to their results, since the energy gap of 16 cm^{-1} in this case is less than the Debye limit in rare gas matrices, the ratio between resonant and single phonon assisted V–V transfer is $\sim 2\times10^2$. Not surprisingly, the hopping probability of excitations is much larger than that of nonresonant energy transfer; or alternatively, the range of nonresonant energy transfer is much shorter than that of hopping and the former will take place either when two excitations are born within the nonresonant transfer range or brought within that range by the hopping mechanism [the range of energy transfer is defined as $(C\tau)^{-6}$, where C is the Förster transfer probability constant defined in Eq. (4), and τ is the excited state lifetime]. The hopping range is dictated by the excited state lifetime of ν_3 while the approach of excitations is determined very strongly by the matrix dilution because of the R^{-6} dependence. Thus to derive macroscopic rate constants based on these microscopic probabilities it is necessary to develop models that take into account concentrations, lifetimes, and energy transfer probabilities.

Finally, it is important to indicate that while a ν_3 excitation is mobile, the mobility of $2\nu_3$ excitations is greatly reduced due to the small $2\nu_3\to 0$ dipole moment matrix element. The $2\nu_3$ state has been directly observed in absorption spectra and its absorption coefficient is approximately two orders of magnitude smaller than that of the ν_3 absorption. Thus the $2\nu_3$ hopping probability, i.e., $P^{2\nu_3\to 0}_{0\to 2\nu_3}$ is expected to be four orders of magnitude smaller than that of the ν_3 hopping probability. Hence, once a molecule is excited in $2\nu_3$, it becomes relatively immobile and further excitation, to populate $3\nu_3$ as an example, is virtually exclusively limited to the arrival of another migratory ν_3 excitation to the site of a $2\nu_3$ excitation. A more direct evidence of this fact was presented in the Moore and Young studies in which the $2\nu_3$ relaxation rate was shown to be independent of concentration while the ν_3 relaxation rate increases as dimers are formed in concentrated matrices.[13]

B. Macroscopic rates

The problem of energy transfer and migration with an R^{-6} law on random or pseudorandom lattices has been treated by numerous authors in a variety of contexts.[21,22] Dubost and Legay have reviewed some of the important literature that applies to the case of vibrational energy transfer.[5,7] Unfortunately, a single analytical solution does not exist for the treatment of the seemingly simple problems of energy migration and transfer in solids. This situation is particularly acute in the case of experiments that span a large concentration range as in the present study. It is therefore necessary to divide the discussion in two, namely (i) macroscopic rates in concentrated matrices and (ii) macroscopic rates in dilute systems. Here, a working distinction between the two regimes is made. In concentrated matrices, hopping rates are fast enough such that the excitation migrates throughout the matrix and hence statistically averaged behavior is observed. In dilute matrices, a nonequilibrium treatment is necessary and kinetic expressions with statistically averaged rate constants cannot be explicitly derived.

In the limit of very fast migration or no migration at all, a simple relation can be derived between the macroscopic rate constant of intermolecular nonresonant transfer, k_f of Eq. (1) and the microscopic probability of the same process. We first consider the case of no mobility at all.

Let N be the total number of sites in the solid, n is the number of guests which occupy randomly distributed substitutional sites, $\delta = n^*/n$ is the fraction of guest molecules excited by the laser with a random distribution. Then the probability that a given site i is occupied by an excited guest molecule is simply $n^*/N = (\delta\cdot n/N)$.[7] The probability that site i has an excited nearest neighbor can be expressed by the continuous nearest neighbor distribution, $P(R,n^*)dR$, introduced by Hertz[24]:

$$P_i(R,n^*)dR = 4\pi R^2\frac{n^*}{V}\exp\left(-\frac{4\pi R^3}{3}\frac{n^*}{V}\right)dR \quad (7)$$

which is the probability that there is an excited molecule within the shell of radius R, thickness dR, and no other excited molecule in the volume of the sphere described by R, assuming an excited state density of n^*/V. If the probability of transfer between two excited molecules separated by R is given by C/R^6, then the average probability of transfer from site i to any other excited nearest neighbor is given by

$$\bar{P}_i = \int \frac{n^*}{N}\frac{C}{R^6}P_i(R,n^*)dR \quad (8)$$

which, after summing over i and dividing by 2 in order to avoid double counting, and dividing by the total volume, gives the average transfer probability $\bar{P}$:

$$\bar{P} = \frac{1}{2V}\sum_i^N\int\frac{n^*}{N}\frac{C}{R^6}P_i(R,n^*)dR \quad (9a)$$

$$= 4\pi \frac{1}{2}\left(\frac{n^*}{V}\right)^2 C \int_{R_0}^{\infty} \frac{e^{-(4\pi/3)R^3(n^*/V)}}{R^4} dR \qquad (9b)$$

which is an infinite series integral that converges very fast for dilute systems. Thus for dilutions used in the reported experiments we can approximate the above integral as

$$\overline{P} = 2\pi \frac{C}{R_0^3}\left(\frac{n^*}{V}\right)^2 . \qquad (10)$$

Note that R_0 is the lower limit of the integral. Since in the present experiments dimers are sites of efficient deactivation, it is necessary to assume R_0 as the third nearest neighbor distance.

In the case of high mobility, the identical expression can be rederived. In this case the assumption is that all occupied lattice sites have equal probabilities of being visited by an excitation. The probability that a given site is a guest is given as n/N; the probability that this site will be excited at any given time is n^*/n. The average probability of having an excited molecule nearby is now given by $n^*/n \cdot P(R,n)dR$. The same transfer probability and summation over $N/2V$ is applicable and now:

$$\overline{P} = \frac{N}{2V}\int_{R_0}^{\infty} \frac{n^*}{n}\frac{n}{N}\frac{C}{R^6}\frac{n^*}{n} 4\pi R^2 \frac{n}{V} e^{-\frac{4\pi}{3}R^3\frac{n}{V}} dR . \qquad (11)$$

This is the same expression as before except n^*/V has been replaced by n/V in the exponent. Then using the same approximation to truncate the series expansion of the integral, the same value for $\overline{P}$ is obtained as in the case of no migration. Thus the cases in which migration will potentially effect the probability for resonant energy transfer will be those between very rapid migration and no migration. Macroscopic rate constants are related to microscopic probabilities according to

$$k = \frac{\overline{P}}{C^n} \qquad (12)$$

in which C is the concentration of reagents and n is the molecularity of the process. Thus the rate constant for the intermolecular V–V transfer process of Eq. (1) is reduced to

$$k = \frac{\overline{P}}{(n^*/V)^2} = 2\pi \frac{C}{R_0^3} . \qquad (13)$$

Numerous approximate expressions for energy transfer rate constants that apply in different limits have been derived previously (see Refs. 7 and 8, for example). The important issue here is that once a rate constant can be derived for microscopic probabilities and fit the requirements of being both time and concentration independent then a simple kinetic treatment is justifiable. Just such a treatment is developed in the next section.

1. Concentrated matrices: Kinetics

In concentrated matrices, where intermolecular separations are small, hopping rates can be fast enough such that energy migrates throughout the matrix. Hence the excited molecular population can be treated as a homogeneous distribution over the entire solid; a function only of the degree of initial excited state population created by the laser. This is a regime in which the excitation transfer probability is large relative to relaxation or nonresonant transfer rates. Thus the situation is analogous to the gas phase where collision rates are large relative to transfer rates and serve as an averaging process. Therefore in analogy with the gas phase, kinetic rate equations can be defined and used to treat the time evolution of the different states. An important criterion to establish the applicability of this limit is the observation of exponential temporal evolutions in the populations of the donor and acceptor states. Another important criterion is the observation of a linear dependence of rates of transfer on the concentration of acceptor states. This occurs when the rate determining step is that of energy transfer to acceptors and is independent of the much faster migration rate.[7]

An exponential rise of population in $2\nu_3$ is seen in Fig. 2. While the concentration dependence will be treated in greater detail, it is important to note that as expected the intercepts of the plots of the energy dependence of the exponential rise rates of $2\nu_3$ shown in Fig. 4 scale with the matrix concentration. At both temperatures, for an approximately fivefold increase in CH_3F concentration there is an approximately fivefold increase in the intercept of the plots. Moreover, it has previously been reported that the ν_3 relaxation rate is also exponential at these concentrations.[11] Thus it can safely be assumed that the system is in the fast migration regime for Xe matrices with $M/R < 10\,000$.

The kinetic model equations that will be considered are

$$CH_3F(\nu_3) + CH_3F(\nu_3) \underset{k_b}{\overset{k_f}{\rightleftarrows}} CH_3F(2\nu_3) + CH_3F(0) , \qquad (14a)$$

$$CH_3F(\nu_3) \xrightarrow{k_r} CH_3F(0) , \qquad (14b)$$

$$CH_3F(2\nu_3) \xrightarrow{k_{21}} CH_3F(\nu_3) . \qquad (14c)$$

The combination of rate Eqs. (14a) and (14b) is commonly encountered in gas phase studies of vibrational energy transfer. The solutions used for the interpretation of such kinetics are usually approximations derived by linearizing the second order equations. The most common approximation is the assumption that the population pumped into the excited states are small relative to ambient populations.[17] Such an assumption cannot be made in cryogenic media. The equilibrium population of the ν_3 excited vibrational states of CH_3F embedded in a 10 K bath is $\sim 10^{-66}$ of the ground state population. In other words, the state is unoccupied. Since there is no ambient population, any induced transient population in the excited states is a large perturbation. An approximate analytical solution is however, still possible in the limit of equilibrium between ν_3 and $2\nu_3$. Since the population in $2\nu_3$ evolves following excitation of ν_3, the rate constant for the transfer of population from ν_3 to $2\nu_3$ must be large in comparison to the ν_3 deactivation rate, $k_f \gg k_r$. In order for the equilibrium assumption to be valid, the rate of population return from $2\nu_3$ to ν_3 should also be large relative to k_r. There are two possible channels for this process: the back rate of Eq. (14a) through k_b, and the direct relaxation mechanism of Eq. (14c) through k_{21}. It follows then, that as

long as $k_b + k_{21} > k_r$, ν_3 and $2\nu_3$ will equilibrate. We first ignore the k_{21} channel and assume $k_f, k_b > k_r$, and derive the approximate expressions for $N_{\nu_3}(t)$ and $N_{2\nu_3}(t)$. Incorporation of k_{21} in the final expressions is straightforward. The validity of these solutions and the limits of their applicability in comparison to numerical solutions is presented in the Appendix. It is worth noting that if k_{21} is insignificant, then the equilibrium assumption will break down at very low temperatures where k_b, the rate of the endothermic step, becomes zero.

Let δ be the fraction of ground state population transferred to ν_3 by the laser pulse. If k_r is small, then, $\delta = N_{\nu_3} + 2N_{2\nu_3}$ holds at all time. Since at these temperatures only the ground state is populated prior to the laser pulse, $N_0 = 1 - N_{\nu_3} - N_{2\nu_3}$ also holds at all times. At equilibrium, the populations are related by the detailed balancing condition:

$$\frac{N^e_{\nu_3}}{N^e_{2\nu_3}} \frac{N^e_{\nu_3}}{N^e_0} = \exp - (\Delta E/kT) = K .$$

These equations can be solved simultaneously to yield the equilibrium populations as a function of laser intensity through δ the anharmonicity gap ΔE and the bath temperature T. For example,

$$N^e_{\nu_3} = (-1 + \{1 - (\delta^2 - 2\delta) \times [4 \exp(\Delta E/kt) - 1]\}^{1/2})/ [4 \exp(\Delta E/kT) - 1] . \quad (15)$$

Following the derivation in Ref. 12, the population rise in $2\nu_3$ can be expressed as

$$N_{2\nu_3}(t) = N^e_{2\nu_3}\{1 - \exp - [N^e_{\nu_3}(4k_f - k_b) + k_b]t\} \quad (16a)$$

and if k_{21} is also included:

$$N_{2\nu_3}(t) = N^e_{2\nu_3}\{1 - \exp - [N^e_{\nu_3}(4k_f - k_b) + k_b + k_{21}]t\} \quad (16b)$$

and finally, as long as the equilibrium assumption holds, $2\nu_3$ will fall at twice the ν_3 fall rate[12]:

$$N_{2\nu_3}(t) = N^e_{2\nu_3}\{\exp - 2k_r t - \exp - [N^e_{\nu_3}(4k_f - k_b) + k_b + k_{21}]t\} \quad (16c)$$

with $N^e_{\nu_3}$ in each case given by the expression in Eq. (15).

The analytical solutions presented above were verified by numerical integration of the equation for the three level model [Eqs. (14a)–(14c)]. The comparison between the exact numerical results and the appropriate analytical expressions Eqs. (16a)–(16c) are represented in the Appendix. As long as intermolecular energy transfer is efficient, $2\nu_3$ will deactivate at twice the ν_3 relaxation rate. Additionally, if the initial excitation does not exceed approximately 10% of the ground state population, ν_3 will relax at a rate of k_r and $2\nu_3$ at $2k_r$. For larger δ, $\delta = \sim 10\%$–50%, the doubling of the ν_3 relaxation rate remains operative, however the ν_3 relaxation rate is reduced relative to k_r as δ is increased. This reduction in ν_3 relaxation rate, which is discussed in more detail in the Appendix, is due to establishment of a cyclical path involving inter- and intramolecular energy transfer [Eqs. (14a)–(14c)] that becomes important when the ν_3 and $2\nu_3$ equilibrium populations are similar. These results are independent of whether ν_3 or $2\nu_3$ is initially excited by the laser pulse.

In the present experiment, $2\nu_3$ relaxes at twice the relaxation rate in all matrices studied. In the experiments of Moore and Young in which $2\nu_3$ in Ar and Kr matrices is initially excited via the 3μ states, the $2\nu_3$ relaxation rate exceeds twice the ν_3 relaxation rate.[13] For this pumping scheme it can safely be concluded that the intermolecular V–V transfer rate is ineffective in establishing equilibrium between the $2\nu_3$ and ν_3 populations. The system directly relaxes to the phonon bath through sequential intramolecular relaxation steps, $2\nu_3 \rightarrow \nu_3 \rightarrow$ ground, in which case the fall rate of $2\nu_3$ is a *direct* measure of k_{21}. In Moore and Young's study of *xenon* matrices, the observed fall rate of $2\nu_3$ in xenon is nearly twice the ν_3 relaxation rate. While this doubling of rates could be coincidental, i.e., $k_{21} \cong 2k_r$, it is not possible to eliminate equilibration of the two states, via intermolecular transfer, as the relaxation mechanism of $2\nu_3$. It is therefore not clear whether k_{21} actually manifests itself as the measured rate. Thus with the possible exception of xenon, the fast equilibrium between ν_3 and $2\nu_3$ does not appear to be present when the system is excited from above. Further evidence for the absence of equilibration in the experiments of Ref. 13 is given by the observed concentration dependence of relaxation rate. The $2\nu_3$ fall is independent of concentration while ν_3 shows a steep increase in relaxation rate in matrices of $M/R < 7000$, indicating an efficient deactivation by transfer to dimers. In the present experiments, where ν_3 is initially excited, *both* ν_3 and $2\nu_3$ exhibit the same concentration dependence. The implication is that, when ν_3 is initially excited, intermolecular transfer is effective in establishing equilibrium between ν_3 and its overtones while when $2\nu_3$ is excited in Kr and Xe, intermolecular transfer is insignificant with respect to direct deactivation.

The obvious difference between the two methods of preparation is the mobility of the initially created excitation. As previously discussed ν_3 excitations are mobile via the hopping mechanism:

$$CH_3F(\nu_3) + CH_3F(0) \rightarrow CH_3F(0) + CH_3F(\nu_3) . \quad (17)$$

However, migration of $2\nu_3$ excitations via

$$CH_3F(2\nu_3) + CH_3F(0) \rightarrow CH_3F(0) + CH_3F(2\nu_3) \quad (18)$$

are very slow and $2\nu_3$ excitations are essentially immobile due to the much smaller matrix element for the $0 \rightarrow 2\nu_3$ transition. Thus when energy migration is required for efficient intermolecular transfer, vibrational equilibrium between ν_3 and $2\nu_3$ can only be established when ν_3 is initially excited as in the present experiments.

It is interesting to note that neither the temperature dependence nor the laser intensity dependence (through δ) are linear for the three level model, Eqs. (14a)–(14c). This is a consequence of the fact that the model contains only three levels and is therefore easily saturated. Yet the observed intensity dependence over a range in which the laser intensity was quadrupled is linear within experimental error. How-

ever, for the limited range of fluences used in the experiments, a satisfactory fit to the data can be realized.

The fluorescence rise in the $M/R = 2500{:}1$ xenon matrix is exponential within experimental error (see Fig. 2). Therefore, the analytical expressions of Eq. (16) are appropriate for the treatment of this data. According to Eq. (16c), the rise rate of $2\nu_3$ should have an intercept given by $k_b + k_{21}$. Whether k_{21} is assumed to be zero or assumed to be the relaxation rate of $2\nu_3$ observed by Moore and Young does not effect the analysis of this data since in either case k_{21} is small enough that it falls within the 10% error range of the intercept values. The reported value of the $2\nu_3$ relaxation rate is 33 ms^{-1} which establishes an upper limit for k_{21}. k_b is thus taken as the intercepts of the fluence dependent curves, 480 ± 50 ms^{-1} and 625 ± 60 ms^{-1}, at 10 and 20 K, respectively. Since the temperatures are known, k_f can be obtained from k_b by detailed balancing. For a given set of k_f and k_b values, δ is then varied to produce a match between the experimental fluence dependence and the fluence dependence predicted by either solution of Eq. (16c) or by numerical integration of the appropriate rate equations. This method of determining δ eliminates any assumptions with respect to the nature and strength of the molecular absorptions of matrix isolated CH_3F. The generated fluence dependence of the rise is shown in Fig. 4. Different δ values, therefore different axes, are necessary to fit the fluence dependence of the rise rates at the two different temperatures. The experimental energy range of 1–2 mJ can then be fit by $\delta = 0.01$–0.022 (1% and 2.2% excitation) at 10 K and by $\delta = 0.02$ and 0.046 (2% and 4.6% excitation) at 20 K. These values and temperature dependence are reasonable in view of the fact that at 10 K the absorption linewidth is inhomogeneously broadened. Therefore, the absorption of the laser is proportional to the ratio of the laser linewidth to the absorption linewidth. As the temperature is increased, the matrix absorption broadens homogeneously, leading to a larger absorption. Ignoring dimerization and assuming that, as expected, the guest/host ratio of the matrix is the same as that of the premixed gas sample, the excited state number densities can be derived from δ and hence the absolute second order rate constants can be determined as $k_f = 5.6(\pm 0.6) \times 10^{-13}$ cc s^{-1} and $1.0(\pm 0.1) \times 10^{12}$ cc s^{-1} at 10 and 20 K, respectively. Using the relationship between k and C derived in Eq. (13), the constant C, which contains in it information about the microscopic probability for energy transfer, can be calculated as 3.8×10^{-35} and 6.7×10^{-35} cm^6 s^{-1} for 10 and 20 K. This calculation was performed using $R_0 = 7.5$ Å, approximately the third nearest neighbor distance. In the vibrational equilibration process, dimers are not involved since dimers are rapidly relaxed. Second nearest neighbors are assumed to dimerize. Thus the closest two CH_3F molecules that can be involved in vibrational equilibration are third nearest neighbors.

These calculated values for C are two orders of magnitude smaller than the resonant hopping rates calculated previously using the expression of Eq. (4) for Förster–Dexter energy transfer. Therefore they are in excellent agreement with the predictions for nonresonant transfer in which the energy defect is within the range of a single phonon.[23]

2. Intermediate dilutions

In samples of intermediate dilution, e.g., $M/R = 13\,000{:}1$, the rise of population in $2\nu_3$ is no longer exponential (see Fig. 5). However, the fluorescence rise time could be satisfactorily fit to a double exponential. It is the rate of the slower of the two exponentials that has been plotted as a function of the laser fluence in Fig. 4. A satisfactory fit to the fluence dependence for this data is not possible within the three level model. As an example, if the intercept is used to obtain k_b and k_{21} and ultimately k_f, no value of δ can reproduce the steep fluence dependence when k_{21} is taken as 33 ms^{-1}. A fit is possible when k_{21} is assumed to be zero. However, in this case δ ranges from 0.1 to 0.4 over the experimental range of fluences from 1–2 mJ. This nonlinear variation of δ with fluence is *inconsistent* with a linear absorption regime. In addition, at these large δ values the system, at least when treated by a three level model, behaves nonlinearly and the fall rate of $2\nu_3$ deviates from twice k_r. This is contrary to experimental observations. The same considerations apply to the data at both 10 and 20 K.

The double exponential exhibited by the population rise and the failure of the three level model to account for the fluence dependence of the rise rate as a function of dilution is a strong indication that in regions of intermediate dilution, the rate of intermolecular energy transfer is influenced by excitation migration. In this dilution regime, excitation migration is not sufficiently fast relative to the nonresonant transfer process for nonresonant transfer to be the rate limiting step in the overall energy transfer process described by Eqs. (14a)–(14c).

It is expected that migration assisted transfer will vanish at zero fluence. Thus at zero fluence, excitation migration will not influence the fluorescence rise time. Therefore the zero intercepts in the fluence dependent curves for the 2500:1 and 12 500:1 samples should be related by the ratio of their dilutions, ~ 5. Indeed, this expectation is borne out, within experimental error, if k_{21} is assumed to be zero. However, if the reported value of k_{21} is used, the deviation of the 10 K intercept from this expectation is outside experimental error.

Migration assisted transfer should be fluence dependent and should show a linear dependence on fluence. This can be seen from the following argument. In the migration assisted transfer regime energy pooling, described by Eq. (1), is expected to occur at specific trap sites. At these trap sites, once an excitation arrives, that excitation remains in this site until another excitation arrives and up pumping occurs. Under these circumstances the arrival of the two excitations is not correlated thus the rate should depend linearly on fluence. This results leads to behavior analogous to a pseudo-first-order gas phase reaction. A phenomenological treatment of the fluence dependence of the rise rate in the intermediate dilution case is then possible. The fluence dependence of the observed rise rate R is treated as a sum of contributions: $R = N^e_{\nu_3}(3k_f - k_b) + k_b + k_{21} + k_m\delta$, i.e., a term corresponding to excitation of $2\nu_3$ in the absence of excitation migration (the zero mobility term) plus a term that takes

into account increasing mobility of excitation with increasing fluence $k_m\delta$. For the first term the values of k_r and δ are taken to be the same as in the 2500:1 sample. The choice of the same δ for the 2500:1 and 13 000:1 matrix is justified by the independence of the linewidth and position on dilution over this concentration regime. From this treatment, a value of $k_m = 1\times10^{-11}$ cc s^{-1} can be obtained. As expected the migration assisted rate constant and migration independent rate constant (which was determined from concentrated samples) are comparable in magnitude at dilutions of 13 000:1 which leads to the observable double exponential behavior of the population rise of $2\nu_3$. Neglect of all other excited vibrational states (except ν_3 and $2\nu_3$) was motivated by the absence of any observable fluorescence from these states. However, a more rigorous justification for their omission from the kinetic model is necessary and will be supplied.

Direct transfer from ν_3 to ν_6 and ν_2/ν_5 is expected to be negligible both on kinetic and thermodynamic grounds. The kinetic argument is based on the fact that the energy gap between ν_3 and ν_6 is outside the Debye limit and hence would require a multiple phonon assisted transfer and thus its probability would be reduced by ~3 orders of magnitude relative to the ladder climbing process.[23] The thermodynamic inhibition is based on the fact that the transition is endoergic by 120 cm^{-1}, and hence inaccessible thermally at cryogenic temperatures. However, it should be recognized that if ν_6 was populated, observing it would be very difficult since ν_6 has a very small transition dipole moment in matrices and is usually not seen in absorption spectra.[15] There are no states in the vicinity of $2\nu_3$ within a single phonon energy gap, moreover any branching from $2\nu_3$ to nearby overtone or combination states would constitute a four quantum transition even if phonon assistance is ignored. Thus the only plausible channel for further vibrational equilibration is that involving $3\nu_3$ in a continuation of the ladder climbing mechanism:

$$CH_3F(2\nu_3) + CH_3F(\nu_3) \rightarrow CH_3F(3\nu_3) + CH_3F(0)\,,$$
$$\Delta E = 32\ \text{cm}^{-1}\,. \qquad (19)$$

The mismatch of energy in this case is within the energy of one phonon and hence the transfer probability is expected to be as efficient as in the first ladder step except for the reduced encounter probability imposed by the immobility of $2\nu_3$ which was discussed above. The $3\nu_3$ population could in principle be observed in either the $3\nu_3\rightarrow2\nu_3$ radiative transition or in $3\nu_3\rightarrow\nu_3$ emission. The first emission could not be directly monitored due to laser scatter while the second could not be distinctly separated from the $2\nu_3\rightarrow\nu_0$ transition as discussed in Sec. III. However, if $3\nu_3$ were populated, it would be expected that it would equilibrate with the $3\,\mu$ states (ν_1, ν_4, $2\nu_2$, $2\nu_5$) through exoergic steps as observed in the gas phase.[17] A significant population does not develop in the $3\,\mu$ states as verified by the absence of any detectable emission in this spectral range. This does not necessarily imply that the $3\nu_3\rightarrow\nu_1/\nu_4$ channel is absent. Even if an infinitely large rate constant is assumed for the transfer from $3\nu_3$ to the rest of the vibrations a steady state population cannot be achieved in the $3\,\mu$ states via this channel. This is a simple consequence of "bottlenecking" by $3\nu_3$ previously discussed in great detail.[17] It should be emphasized though, that while equilibrium populations of the $3\,\mu$ states cannot be achieved through this channel, the $3\nu_3$ population can be effectively depleted. Thus in the absence of a steady state population in $3\nu_3$, very little population is expected to climb the ν_3 ladder up to $4\nu_3$ and higher overtones. In addition to the depletion of population in these higher overtones by coupling to the rest of the molecular vibrations the energy pooling mechanism would now require multiphonon assistance due to the increase in energy gap of the ladder climbing process.

In their LIF experiments, Moore and Young excited different $3\,\mu$ states in CH_3F and in all cases observed instantaneous population of $2\nu_3$.[13] This indicates that intramolecular V–V transfer between the different modes of CH_3F can be very effective in the case of exoergic transfer, and hence justifies the argument that $3\nu_3$ could provide the doorway for populating the rest of the vibrations via intramolecular transfer.

The temperature dependence of the experimental $2\nu_3$ rise rate is shown in Fig. 3. A simple linear dependence is observed which is surprising in view of the numerous temperature effects that are expected to contribute to the rise rate. The kinetic effect is due to the microscopic reversibility relation between k_f and k_b and the temperature dependence of the ν_3 equilibrium population. These can be summarized by recasting the rate of rise given in Eq. (16c) as

$$R = k_f\left[4N^e_{\nu_3} + (1-N^e_{\nu_3})e^{-\Delta E/kT}\right]. \qquad (20)$$

Both k_f and k_{21} are rate constants of phonon assisted processes and are therefore expected to be proportional to the temperature dependent phonon population. This can be accounted for by explicitly including the single phonon population statistics:

$$R \propto \frac{\left[4N^e_{\nu_3} + (1-N^e_{\nu_3})e^{-\Delta E/kT}\right]}{1-e^{h\nu/kT}} \qquad (21)$$

in which $h\nu$ is the energy of the phonon necessary to overcome the anharmonicity mismatch between $\nu_3+\nu_3$ and $2\nu_3$. Therefore $h\nu = \Delta E = 16$ cm^{-1}. A linear dependence on temperature is predicted by Eq. (21), however the predicted slope is too steep to match the experimental points. In the range of temperatures studied the absorption linewidths change by a factor of 10, therefore Förster transfer probabilities, hence k_f, will also change. Finally, a change of absorption linewidth and line shape also implies a change in the absorption, hence the excited state population δ and $N^e_{\nu_3}$. Thus in view of all the known sources for the variation of rise rates with temperature, the observed linear dependence contains no more information other than the obvious conclusion that these nonlinear contributions cancel out to yield an overall linear dependence.

Finally, it is possible to interpret the observed host dependence of intermolecular V–V rates. In the fast migration regime, for a given mole fraction of excited states, the intermolecular rate constant should scale as $n^{-4}d^{-6}$ (n = index of refraction, d = nearest neighbor distance[7]). Thus the rise rates in $2\nu_3$ should scale as 4.1:2.4:1 in Ar:Kr:Xe. Though it is difficult to make an exact comparison of rates obtained in different matrices since the fraction of molecules excited by the laser is not directly measured, the rise rates obtained under similar conditions should not deviate substantially from this ratio. The observed rise rates in the different ma-

trix hosts at 10 K and 1 mJ excitation energy, were: $1200 \pm 200\ ms^{-1}$ in Ar ($M/R = 8500$), $750 \pm 50\ ms^{-1}$ in Kr ($M/R = 8000$), $235 \pm 20\ ms^{-1}$ in Xe ($M/R = 10\,000$). Thus without making any corrections for linewidths, absorption coefficients, or concentrations, a ratio of 5.1:3.2:1 is observed; in reasonable agreement with the expected ratio.

3. Dilute matrices

At intermediate dilutions, $M/R = 10\,000$–$30\,000$, where the average separation between CH_3F molecules is 20–30 Xe atoms, the rise of population in ν_3 is clearly not a single exponential. A single and double exponential analysis of the rise is shown in Fig. 5 for data taken from a sample of $M/R = 13\,000$. The deviation from a single exponential rise is even more significant in the very dilute samples. In Fig. 6 signals taken from $M/R = 15\,000$ and $60\,000$ are shown. While the data in the intermediate dilution regime might initially appear to have a double exponential rise, on further examination it is found that the first, fast part of the rise is not exponential. Confirming this is the fact that an iterative Guggenheim analysis of the data (which treats the data as an exponential or sum of expotentials) was often divergent, indicating that the fast part is not exponential. A nonexponential time evolution at early times and in dilute matrices is expected and could in principle, be treated by an extension of the donor-acceptor transfer expressions of Inokuti and Hirayama.[25] However, the time response of the detection system used in this study does not allow for such a detailed analysis. Thus relative amplitudes of the fast and slow rising signals will be considered.

As previously indicated, an exact analytical treatment of excitation migration and transfer in this very wide range of concentrations, $M/R = 10\,000$–$100\,000$, is not possible. However there exist many numerical treatments of this problem usually through random walk models generated by Monte Carlo methods. Additionally, a simplified and intuitive expectation for the time evolution of population in $2\nu_3$, in the very dilute systems can be obtained. In the situation where the energy migration through resonant hopping is slow and hence determines the rate of population transfer to $2\nu_3$, a bimodal distribution of transfer probabilities is expected. One mode is due to the distance averaged long range V–V transfer among excited pairs, which are created by the laser, near enough to each other such that V→V transfer can occur on the time scale of the decay of a ν_3 quantum yet far enough from other CH_3F molecules that sampling of a large number of CH_3F molecules is unlikely. The second mode comes from excited CH_3F molecules that are distributed close enough to other CH_3F molecules that significant excitation migration occurs *before* the nonresonant energy transfer step. The first process will be weighted by R^{-6} and strongly biased by the excitation pairs created in proximity of each other. This distribution is in turn strongly biased by deviations from statistical distributions of intermolecular distances and hence by the matrix preparation techniques such as annealing, deposition temperature, etc. Thus it is expected that energy transfer rates due to this initial distribution of pairs of excited CH_3F molecules will be second order in the excited state population while the slower part of the rise will be determined by the migration rate and hence it will be first order in the excited state population. Thus a phenomenological treatment of the amplitudes of the fast and slow rise processes as a function of excited state population and therefore excitation energy should follow the relation

$$\frac{A_{\text{fast}}}{A_{\text{total}}} = \frac{A_{\text{fast}}}{A_{\text{fast}} + A_{\text{slow}}} = \frac{aI^2}{aI^2 + bI} = \frac{a}{a + b/I}. \quad (22)$$

The ratio of the amplitudes of the bimolecular process to that of the total amplitude should asymptotically reach unity as the excitation energy is increased. This expectation is well-borne out as indicated in Fig. 7. It is also clear that the matrix history, such as annealing, is a significant factor in determining the relative amplitude of the two rises. This is a dramatic demonstration that migration on pseudo random lattices with an R^{-6} law is, in contrast with Markov processes, a system with memory.

A very simple Monte Carlo model serves as a test of the validity of the above interpretation. In the simplest of these models, we consider a two dimensional ordered lattice as in Fig. 12, where each circle represents an occupied lattice site. Two positions on the lattice are selected at random, representing two ν_3 excited molecules—one stationary, one migratory. The migration direction is chosen with a random number generator. A unity probability for a hop is assumed when the destination position is occupied by a ground state molecule. If the destination position is occupied by the ν_3 excited stationary molecule, the probability of a hop is weighted by a fraction P_T. In addition, a spontaneous decay probability P_D is assumed. All probabilities are referenced to the unity resonant hopping probability. Three representative cases are shown in Fig. 13. The concentrated regime which is characterized by fast hopping compared to deactivation or nonresonant transfer, is modeled by assuming $P_D = 0$ and $P_T = 1/9$ in the 9×9 lattice. This is the top trace in Fig. 13. The full scale of the trace is 400 time steps within which all transfer is complete and the time evolution of transfers is

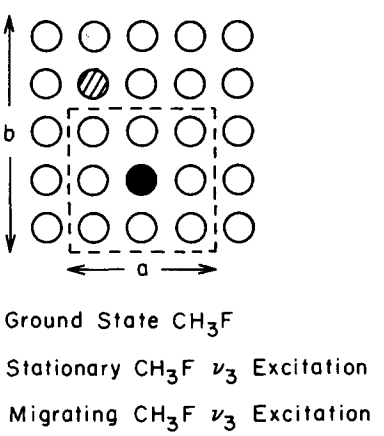

FIG. 12. The two dimensional array used for the Monte Carlo simulation. The open circles mark CH_3F sites, the filled circle marks a stationary ν_3 excitation and the cross-hatched circle a migrating ν_3 excitation. The dilution effect can be simulated by increasing the deactivation probability, relative to the transfer probability. The fractional excitation (fluence dependence) is simulated by changing the number of unexcited sites (b) and the range of energy transfer is defined by (a).

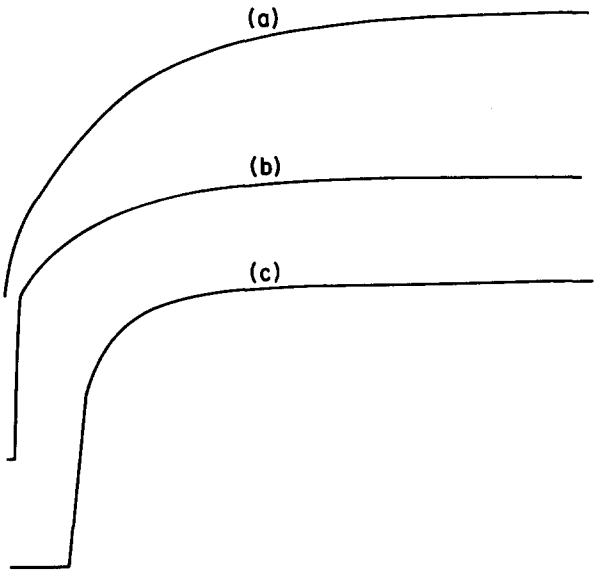

FIG. 13. $2\nu_3$ populations simulated by the Monte Carlo routine in a 9×9 array ($b=9$). The top curve (a) corresponds to the concentrated regime where transfer is slow relative to hopping probabilities. This was simulated by assuming $P_T=1/9$ and $P_D=0$. The middle curve (b) corresponds to intermediate dilution where the transfer probability is comparable to hopping. Simulated by assuming $P_T=1$, $P_D=0$. The lower trace (c) corresponds to the dilute matrix where deactivation competes with transfer and hopping probabilities. Simulated by assuming $P_T=1$, $P_D=0.5$ Each curve is the result of 1000 walks. The abscissa is in units of hop steps. The fall scales are (a) 400 steps, (b) 130 steps, (c) 30 steps.

exponential. The intermediate dilution regime is characterized by comparable transfer and hopping probabilities and both processes are significantly faster than the deactivation rates. This regime is modeled by assuming $P_D=0$ and $P_T=1$—middle trace in Fig. 13. The full time scale for this trace is 130 steps. A bimodal distribution for $2\nu_3$ excitation is clear. The relative amplitudes in this case are simply determined by the initially generated positions. When the two excitations are born as neighbors then they have the chance of direct transfer or else the excitation hops away and migration must bring it together. When they are not born as neighbors, migration is necessary. The final example the dilute case, is represented by $P_D=0.5$ and $P_T=1$. In this case, all transfer is completed within the first ten time steps. If the pairs are created far from each other, the chances of their meeting prior to deactivation is very small. Therefore only pairs created as neighbors may transfer energy to create $2\nu_3$ and this takes place at early times or not at all.

This simple model seems to accurately represent the essence of the observed experimental time evolution of $2\nu_3$ as a function of concentration as shown in Fig. 6. In the 60 000:1 sample only a fast rise can be observed. This implies that most of the population decays prior to transfer to $2\nu_3$ which is also borne out by the great reduction in S:N vs more concentrated matrices. It is, however, curious that even at $M/R=60\,000$ the decay rate of $2\nu_3$ is exponential with a rate twice that of ν_3 deactivation. This implies that on the relaxation time scale, vibrational equilibrium is established between $2\nu_3$ and ν_3. The vibrational temperature in this case is not given by the initial excited state population, since deactivation is competitive with energy transfer on the V–V time scale. Thus the system will equilibrate at a greatly reduced vibrational temperature which can be estimated by assuming that the effective excited state population is given by the initial excited state population created by the laser multiplied by the ratio of the time over which a flat top on the signal persists (from $t=0$ to the beginning of the exponential portion) to the relaxation time. In the case of the 60 000:1 matrix, the flat top persists for $\sim10\,\mu$s while the relaxation time is $50\,\mu$s therefore only $\sim80\%$ of the initial ν_3 excitation comes into equilibrium.

V. CONCLUSIONS

When the lowest frequency fundamental, ν_3, of matrix isolated CH_3F is excited, energy is transferred by an intermolecular vibration–vibration energy transfer process primarily to the $2\nu_3$ overtone. The establishment of vibrational thermal equilibrium in the cold phonon bath is the driving force for this process which is exothermic due to the anharmonic ν_3 manifold. The V–V transfer proceeds through long range dipolar interactions. Two types of energy transfer could be identified: a resonant hop and a nonresonant transfer. The first does not change state populations, however, it serves as a mechanism for the migration of ν_3 excitation of CH_3F molecules in the solid. The Förster energy transfer formalism is applicable in this case and the hopping probability can be evaluated since all the necessary parameters are known from spectroscopic studies. Nonresonant transfer proceeds among ν_3 excited molecules brought in proximity by the hopping process. The nonresonant transfer proceeds via phonon assistance. The phonon assisted transfer probability was obtained from fluence dependence studies in concentrated matrices where the fast migration assumption with respect to ν_3 excitation with verified to be valid. The phonon assisted intermolecular V–V transfer probability constants in Xe are 3.8×10^{-35} and 6.7×10^{-35} $cm^6\,s^{-1}$ at 10 and 20 K, respectively. The associated rate constants increase in the order Ar:Kr:Xe with a ratio of 1:3.2:5.1. At intermediate dilutions, a migration assisted energy transfer can clearly be identified. It is clearly established that there is a need for fast migration via intermolecular transfer, which proceeds when ν_3 is excited but not when $2\nu_3$ is excited.

In dilute matrices, in which the fast migration assumption breaks down, the population rise in $2\nu_3$ clearly shows two contributions: A fast nonexponential rise, followed by a slower exponential rise. The sources of these two contributions could be verified by simple Monte Carlo simulations. The fast nonexponential rise is due to transfer among pairs of excitations created in near proximity of each other by the laser pulse while the slow rise is due to nonresonant transfer of excitations brought into proximity via the migration process. This could also be verified experimentally. The amplitude of the first rise shows a second order fluence dependence while the second part has a linear dependence. In this

case the entire excited state population created by the laser pulse does not come into equilibrium. However, a well-defined vibrational temperature evolves on the relaxation time scale evidenced by the observed exponential decays in matrices as dilute as 100 000:1. Whether the equilibrium is among *clusters of molecules* or the entire matrix could not be verified. However, it could be verified that energy migration is nondispersive in nature since the system retains memory—the observed rise rates and amplitudes are subject to the matrix history, as shown by annealing experiments. Further studies and more sophisticated models are necessary to obtain a more detailed picture of the energy transfer and migration processes in these dilute matrices.

ACKNOWLEDGMENTS

We would like to acknowledge support of this research by the Donors of the Petroleum Research Fund administered by the American Chemical Society via Grants No. 1542-G5 (VAA) and No. 11112-AC6 (EW) and by the National Science Foundation under Grant No. CHE85-06957. One of us (W J) acknowledges a fellowship from the Deutsche Forschungsgemeinschaft.

APPENDIX

The analytical solution for the three level model:

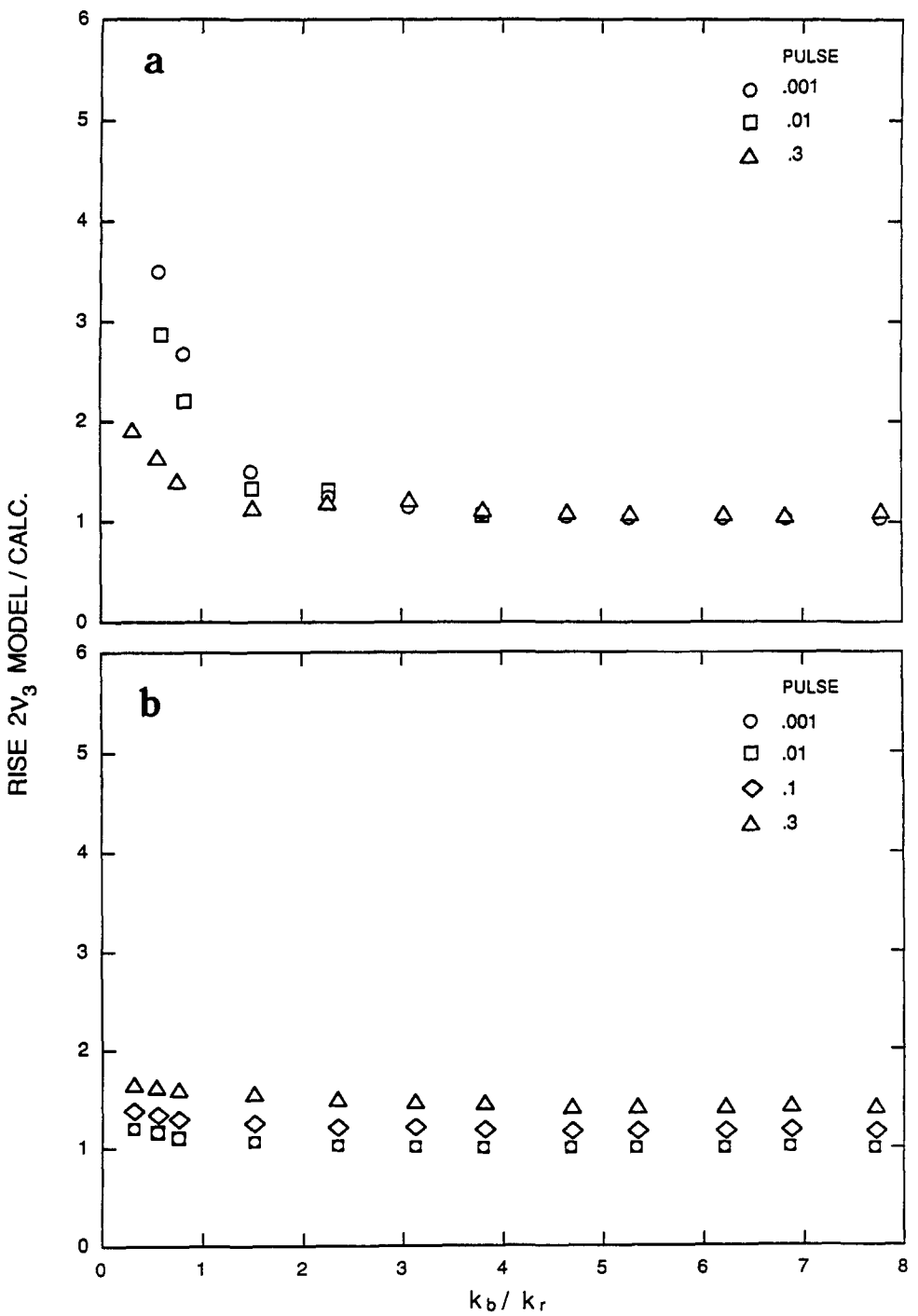

FIG. 14. (a) A plot of the rise rate of $2\nu_3$ calculated from the analytical solution of Eqs. (A1)–(A3) divided by the rise rate of $2\nu_3$ calculated from numerical integration of Eqs. (A1)–(A3). The abscissa is k_b/k_r where these rate constants again refer to Eqs. (A1)–(A3). These calculations are performed for three different pump pulses; $\delta = 0.001$ (○), $\delta = 0.01$ (□), and $\delta = 0.3$ (△). (b) Same plot as in (a) except now k_{21} is set equal to $2k_r$.

$$CH_3F(\nu_3) + CH_3F(\nu_3) \underset{k_b}{\overset{k_f}{\rightleftarrows}} CH_3F(2\nu_3) + CH_3F(0)\,, \tag{A1}$$

$$CH_3F(2\nu_3) \xrightarrow{k_{21}} CH_3F(\nu_3)\,, \tag{A2}$$

$$CH_3F(\nu_3) \xrightarrow{k_r} CH_3F(\text{ground}) \tag{A3}$$

was presented in the main text, Eq. (11). The solution was based on the assumption of fast equilibrium between ν_3 and $2\nu_3$. This limit is achieved when the V–V rate constant (k_f, k_b, and k_{21}) are large relative to k_r. In this section the limits of applicability of the previously presented approximate solutions are considered. To achieve this comparison, Eqs. (A1)–(A3) were numerically integrated and the time dependence of the populations of the states were analyzed as exponentials. When ν_3 is initially excited, the $2\nu_3$ population is analyzed as an exponential rise and an exponential fall, while ν_3 is analyzed as a double exponential fall. When $2\nu_3$ is directly excited, $2\nu_3$ is analyzed as a double fall while ν_3 is analyzed as a rise and a fall. This treatment is approximate, since the time evolution of the population in a given state need not be strictly exponential. In fact, a second order equilibration mechanism would be expected to exhibit a time dependence which could more appropriately be described as

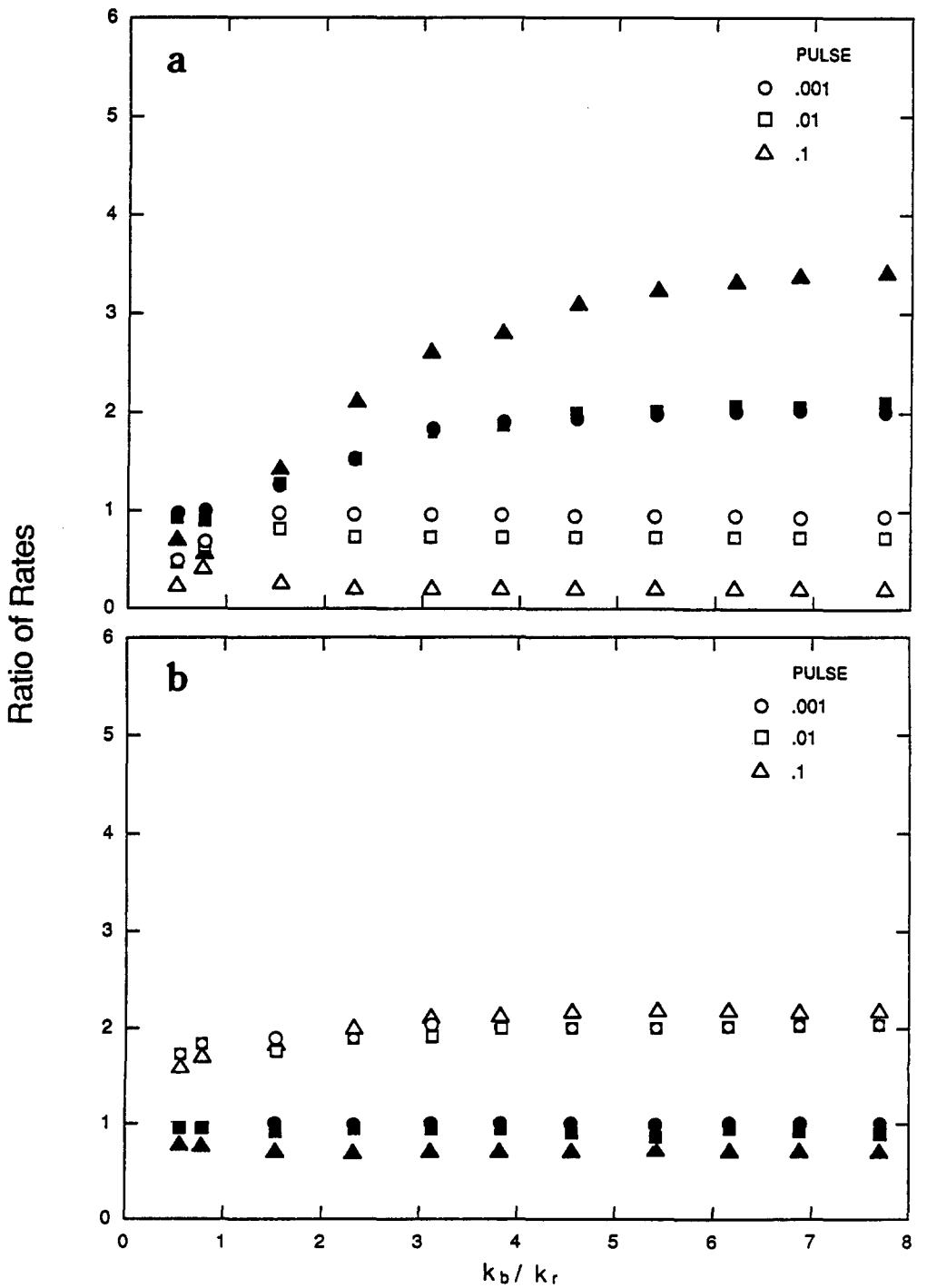

FIG. 15. (a) The filled points are the ratio of the relaxation rates of $2\nu_3$ divided by the relaxation rate of ν_3 plotted against k_b/k_r for various pulse energies. In each case the relaxation rates come from numerical solutions of Eqs. (A1)–(A3). The open points depict the variation of the fall rate of ν_3 obtained from the numerical solution of Eqs. (A1)–(A3) divided by k_r plotted vs k_b/k_r for various values of the excitation pulse. (b) Same plot as in (a) except with $k_{21} = 2k_r$.

a hyperbolic tangent. However, since the experimental data are treated satisfactorily as exponentials, it is useful and consistent to treat the numerical data in a similar fashion.

Two cases are treated separately, the case of $k_{21} = 0$ and $k_{21} = 2k_r$. The parameter that is varied in each case is k_b/k_r. Since k_f is always larger than k_b, a large value of k_b/k_r assures equilibration of ν_3 and $2\nu_3$. The most severe situation with respect to equilibration is at the lowest temperature. Since the relation between k_f and k_b can always be determined at a given temperature by detailed balance, the numerical calculations were carried out at one temperature, 10 K, which is the lowest temperature at which experiments were performed. In Fig. 14(a), the validity of the approximate expression for the rise rate is tested at different levels of excitation for $k_{21} = 0$. As long as $k_b > 2k_r$, the solution is exact within experimental error (10%). As k_b is reduced in magnitude, the approximate solutions start to deviate from the exact solution. The deviations are larger for a given k_b/k_r ratio for smaller levels of excitation. This is due to the fact that the overall equilibration rate contains a term given by $k_f N_{\nu_3}$. Hence the V–V rates are larger for larger initial pulses. Interestingly, in the regime of greater nonlinearity in the kinetic equations, the equilibrium assumption for ν_3 and $2\nu_3$ is better and thus the approximate solution is *closer* to the exact solution than in a regime of greater linearity.

In Fig. 14(b), the same comparison is made as in Fig. 14(a) except now k_{21} is set equal to $2k_r$. The approximate solution is now valid over a larger range of k_b/k_r than before. In the limit of $k_b/k_r = 0$, the deviations from the exact solution are smaller than in the case where $k_{21} = 0$. However, note that for very large values of δ (30% pump) the rise rate of $2\nu_3$ is 25% larger than predicted by the analytical expression. This deviation in rise rate does not occur for small values of δ. The deviation is a manifestation of the effect of the cyclical deactivation pathway inherent in the kinetic model. The path involving direct deactivation of $2\nu_3(k_{21})$ populates ν_3 at the expense of $2\nu_3$. An increase in the population of ν_3, in turn, causes an increase in the effective rate of population of $2\nu_3$ since an increase in ν_3 population necessitates a larger k_f. Thus, effectively, the pathway for direct deactivation of $2\nu_3$ accelerates the rise rate of $2\nu_3$!

In Fig. 15(a), the validity of the approximate expressions for the relaxation of ν_3 and $2\nu_3$ is tested. The upper curves correspond to the fall rate of $2\nu_3$, divided by the fall rate of ν_3 where both rates have been obtained from the numerical solutions. A doubling of relaxation rates for $2\nu_3$ vs ν_3 would thus produce a value of two for this quotient. For mild pumping, (1%–10%), a doubling of rates is observed for $k_b \geqslant 3k_r$. However, for smaller values of k_b the relaxation rate of $2\nu_3$ is less than twice the ν_3 relaxation rate. Note that the doubling of relaxation rates does not occur for larger values of δ for all values of k_f/k_b. This again is a consequence of the nonlinearity of the kinetics. Therefore, a doubling of relaxation rates will not occur for high degrees of excitation ($\delta \geqslant 5\%$).

In the lower curves of Fig. 15(a), the fall rate of ν_3, from the numerical solutions, is divided by k_r and plotted vs k_b/k_r. A value of unity for this ratio is observed for small excitation levels, i.e., ν_3 relaxes at k_r. However, for high levels of excitation, the ν_3 fall rate is *reduced*. This effect can be understood by realizing that at high levels of excitation a significant amount of the population pumped into ν_3 does not reside in ν_3 at vibrational equilibrium; it has been pumped up to $2\nu_3$ via the V–V equilibration process. Thus only a fraction of the initially excited molecules have a vibrational deactivation pathway open to them and the effective deactivation rate is less than k_r.

Finally, in Fig. 15(b) the same parameters are considered as in Fig. 15(a) but with $k_{21} = 2k_r$. Under these circumstances, a doubling of relaxation rate for $2\nu_3$ vs ν_3 is observed even for $k_b = 5k_r$ and for values of δ as large as 0.1 (10% pump). The fall rate of ν_3 deviates from k_r only for large values of δ. For $\delta = 1$, the largest deviation of the fall rate vs k_r is $\sim 35\%$. Note that the deviation of the fall rate of ν_3 from k_r increases as k_b increases, again indicating that the magnitude and time scale for depletion of ν_3 via pumping of $2\nu_3$ becomes significant in this limit. Hence the rate of relaxation of ν_3 is reduced.

[1] *Inert Gases: Potentials, Dynamics and Energy Transfer in Doped Crystals*, Vol. 34 in Springer Series in Chemical Physics edited by M. L. Klein (Springer, Berlin, 1984).
[2] M. Poliakoff and E. Weitz, Adv. Organomet. Chem. **25**, 277 (1986).
[3] T. A. McDonald and J. S. Shirk, J. Chem. Phys. **77**, 2355 (1982).
[4] M. Perttilä, J. Murto, A. Kivinen, and K. Turunen, Spectrochim. Acta Part A **34**, 469 (1978); J. Pourcin, G. Davidovics, H. Bordot, L. Abouaf-Marguin, and B. Gauthier-Roy, Chem. Phys. Lett. **74**, 147 (1980); L. Homanen and J. Murto, *ibid.* **85**, 322 (1982); H. Takeuchi and M. Tasumi, Chem. Phys. **70**, 275 (1982).
[5] J. Dubost, in Chap. 4 of Ref. 1.
[6] L. E. Brus and V. E. Bondybey, in *Radiationless Transitions*, edited by S. H. Lin (Academic, New York, 1980).
[7] F. Legay, in *Chemical and Biochemical Applications of Lasers*, edited by C. B. Moore (Academic, New York, 1977), Vol. II.
[8] D. J. Diestler, in *Radiationless Processes in Molecules and Condensed Phases*, Vol. 15 in Topics in Applied Physics, edited by K. F. Fong (Springer, Berlin, 1976).
[9] J. M. Wiesenfeld and C. B. Moore, J. Chem. Phys. **70**, 930 (1979); L. Young and C. B. Moore, *ibid.* **81**, 3137 (1984).
[10] A. D. Abbate and C. B. Moore, J. Chem. Phys. **82**, 1263 (1985).
[11] B. Gauthier-Roy, L. Abouaf-Marguin, and F. Legay, Chem. Phys. **46**, 31 (1980): B. Gauthier-Roy, Thesis, Universite de Paris Sud (Centre d'Orsay), 1980.
[12] V. A. Apkarian and E. Weitz, Chem. Phys. Lett. **76**, 69 (1980).
[13] L. Young and C. B. Moore, J. Chem. Phys. **76**, 5869 (1982).
[14] M. D. Fayer, Annu. Rev. Phys. Chem. **33**, 63 (1982).
[15] V. A. Apkarian and E. Weitz, J. Chem. Phys. **76**, 5796 (1982).
[16] E. A. Guggenheim, Philos. Mag. **2**, 538 (1976).
[17] V. A. Apkarian and E. Weitz, J. Chem. Phys. **71**, 4349 (1979).
[18] V. A. Apkarian, Ph.D. thesis, Northwestern University 1981.
[19] C. E. Treanor, J. W. Rich, and R. G. Rehm, J. Chem. Phys. **48**, 1798 (1968).
[20] R. D. Levine and J. Manz, Chem. Phys. **33**, 151 (1978).
[21] K. Godzik and J. Jortner, J. Chem. Phys. **72**, 4471 (1980); J. Klafter and A. Blumen, *in AIP Conference Proceedings No. 109*, edited by M. F. Schlesinger and B. J. West (AIP, New York, 1982).
[22] V. K. S. Shante and S. Kirkpatrick, Adv. Phys. **20**, 325 (1971); R. Kopelman, p. 297 of Ref. 8; I. Rips and J. Jortner, Chem. Phys. **99**, 207 (1985).
[23] A. Blumen, S. H. Lin, and J. Manz, J. Chem. Phys. **69**, 881 (1978).
[24] F. Hertz, Math. Ann. **67**, 381 (1969).
[25] M. Inokuti and F. Hirayama, J. Chem. Phys. **43**, 1978 (1965).